SAND80-2007
Unlimited Release
UC-21

The T-3 Electron-Beam-Excited Laser System

Raymond A. Klein

Prepared by Sandia National Laboratories, Albuquerque, New Mexico 87185
and Livermore, California 94550 for the United States Department of Energy
under Contract DE-AC04-76DP00789

Printed February 1981

Sandia National Laboratories

F 2900-Q(3-80)

DISCLAIMER

Issued by Sandia Laboratories, operated for the United States Department of Energy by Sandia Corporation.

PAGES 1 to 2

WERE INTENTIONALLY

LEFT BLANK

SAND80-2007
Unlimited Release
Printed February 1981

UC-21

THE T-3 ELECTRON-BEAM-EXCITED LASER SYSTEM*

Raymond A. Klein
Sandia National Laboratories
Albuquerque, New Mexico 87185

ABSTRACT

A laser system specifically designed to study the kinetics of electron-beam driven systems is described. Details of the system are given along with measurements of the electron-beam uniformity and deposition in the laser medium. Some HF laser results obtained with this system are also given.

---

*This work partly funded by the Air Force Weapons Laboratory, Kirtland Air Force Base, Project #80-102.

Printed in the United States of America

Available from
National Technical Information Service
U. S. Department of Commerce
5285 Port Royal Road
Springfield, VA 22161

Price: Printed Copy $4.00 ; Microfiche $3.00

CONTENTS

FIGURE CAPTIONS

I. Introduction

The T-3 facility was developed so that detailed kinetic/optical studies could be performed on an electron-beam-initiated HF/DF chemical laser. The basic idea was to develop a well characterized system so that detailed comparisons could be made with Sandia's laser code predictions. These comparisons would enable problem areas in the code to be more precisely identified. One of the major requirements of the system was that the electron deposition in the laser mixture be well characterized, both as to the uniformity and the amount of energy deposited. Another requirement was that the laser cell be so constructed that many diagnostics could be used during the same experiment. Some of the measurements planned for the T-3 device were to determine the F atom concentration produced by the electron beam, to measure the F_2 disappearance and hence the overall reaction time in H_2/F_2 gas mixtures, to determine the HF build up caused by prereaction of the H_2 and F_2 and to determine small-signal gains on a number of laser lines.

This report will give details of the electron-beam system, including the design and construction of the laser cell. In addition, electron-beam deposition measurements and some preliminary laser measurements will be included.

II. General Design of the System

A schematic representation of the T-3 system is shown in Fig. 1. The electrons produced in the accelerator enter the laser cell transverse to the optical axis so that uniform excitation can be achieved. Hibachi structures which support the foils on both sides of the cell allow operation up to pressures of 5 atm. A burst diaphragm is used to prevent the over pressure from the $H_2 + F_2$ reaction from damaging the laser cell. The laser

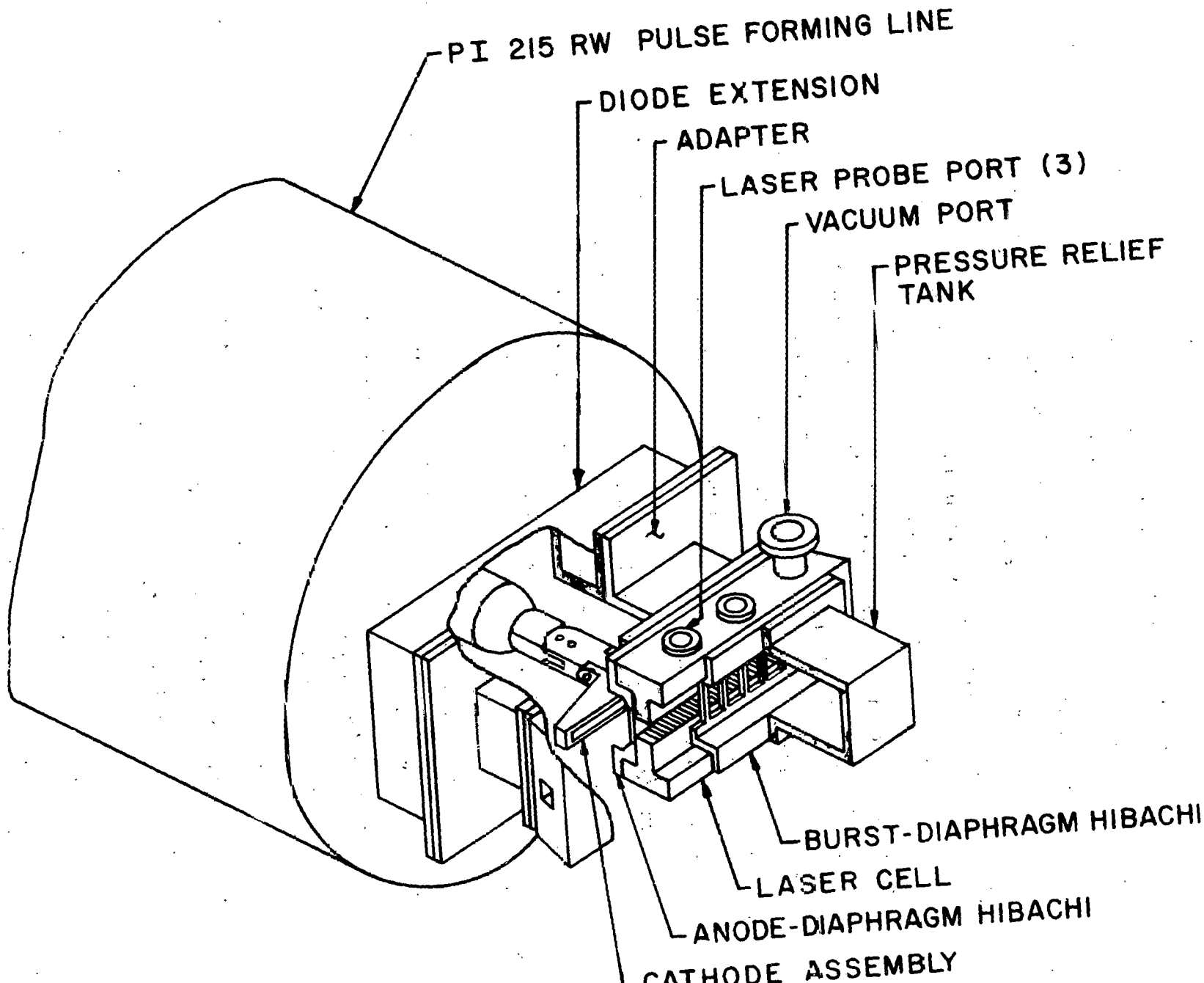

Fig. 1. Cutaway drawing of the T-3 laser system.

cell is also equipped with three vertical transverse laser probe ports so that optical measurements can be made transverse to the optical axis.

The electron-beam accelerator[1] has a pulse width of 50 nsec and operates at voltages up to 520 kV with currents up to 40 kA. The machine was originally designed to be a 0.5 J pulse-per-second KrF laser.[2] The original machine has been modified for single pulse operation for the T-3 laser system.

A gas handling and pumpout system, similar to one previously described,[3] is used with this system. Its function is to evacuate the laser cell to a base vacuum of 10^{-5} Torr and then fill the cell to various pressures of F_2, O_2, H_2, SF_6, and HF gases. The gas handling system is remotely controlled so that personnel need not run the risk of exposure to the caustic, explosive gas mixtures.

A photograph of the system is shown in Fig. 2. The moveable cart in the foreground contains vacuum pumps and F_2 traps. Optics mounted to an optical bench are used to steer the probe laser beam into the cell for optical absorption measurements. The entire room, which contains the electron-beam machine and laser cell, is enclosed with concrete blocks and a lead door for x ray shielding.

III. Electron-Beam Accelerator

The accelerator is a Physics International machine, Model PI 215WR. As was previously mentioned, this device was originally developed and used extensively for a 0.5 J, 1 pps, KrF laser at Los Alamos Scientific Laboratories. Upon its return to Sandia, the machine was rebuilt and modified for operation with the T-3 system. The modifications included a new triggering circuit and a new diode design. Since the accelerator is a commercial device, only a brief description will be given of its

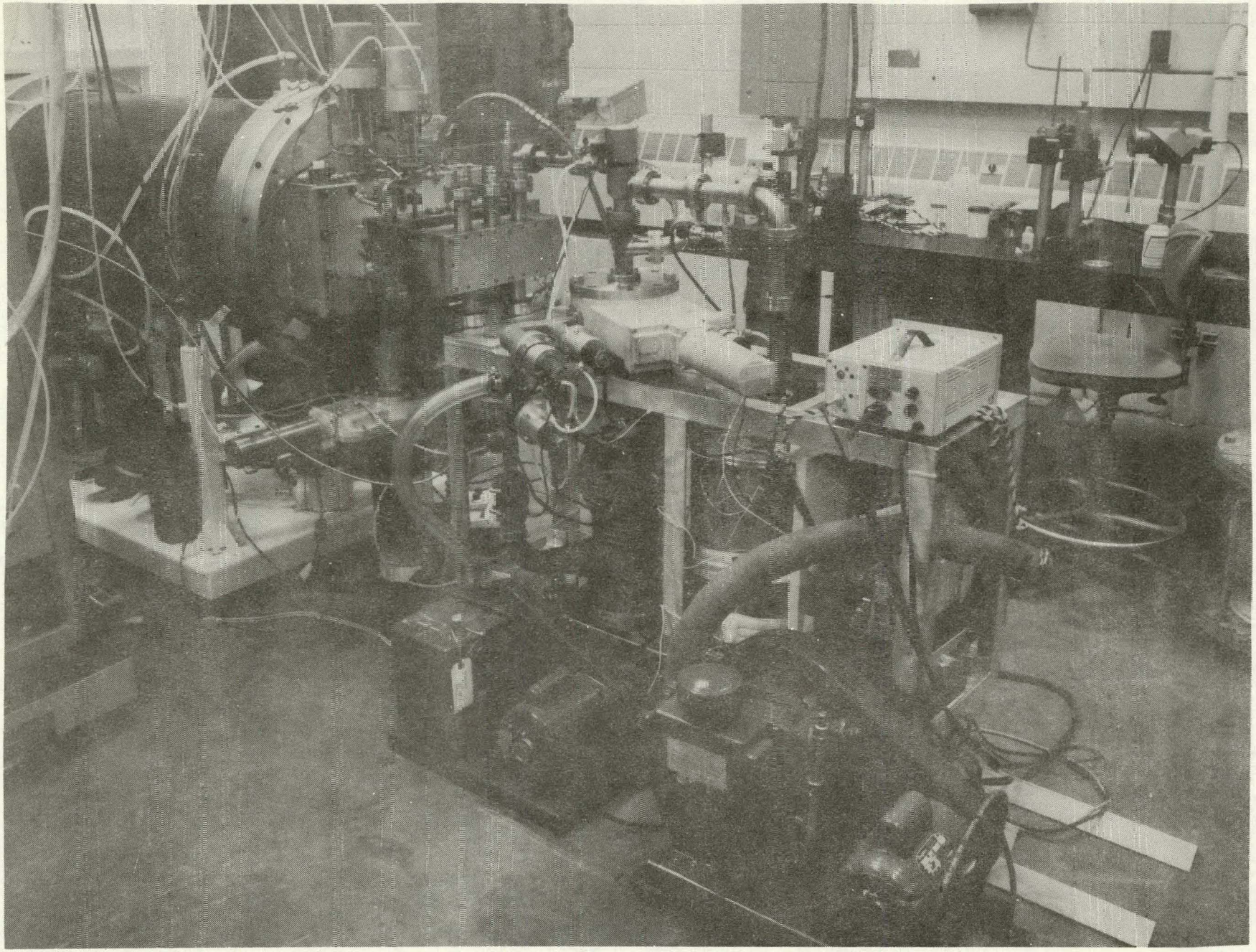

Fig. 2. Photograph of experimental setup.

operation; however, modifications to the machine will be described.

A block diagram of the accelerator is shown in Fig. 3. The Marx generator is immersed in oil to prevent electrical breakdown. The Marx is DC charged to a maximum of 38 kV/stage. There are 15 stages whose series capacity is 3.2 nF. At a charge voltage of 38 kV, the Marx generator stores approximately 2 kJ. The energy from the Marx charges a coaxial waterline, whose length determines the pulse width of the accelerator. The length of the line is 84 cm, corresponding to an electron-beam pulse width of 50 nsec. The energy from the coaxial line is transferred to the diode by a self-triggering high-pressure gas switch. The pulse applied to the diode has an amplitude approximately half that of the switched voltage and a duration twice the transit time of the coaxial line. The operating SF_6 gas pressure of the main switch varies from 60 psi for a 30 kV Marx charge to 90 psi for a charge voltage of 38 kV. These pressures were determined by obtaining a self-breakdown curve (voltage versus SF_6 pressure) after the machine was rebuilt.

The original trigger circuit of the Marx was completely replaced. Before replacement, the trigger was a major source of problems with the machine. The new trigger system for the T-3 system incorporated a TC-70 pulse generator[4] to trigger the first three stages of the Marx. This trigger system reduces the time jitter of the Marx generator to a few nsec.

The original diode had a 5 cm x 30 cm cathode surface and was used to excite a volume of 6.35 cm x 6.35 cm x 30 cm long. The current density entering the laser chamber was approximately 110 A/cm^2. For chemical laser research, a current density of approximately 500 A/cm^2 was required; therefore, a new smaller area diode was designed. Also, it was desired to make the impedance of the diode about 15 ohms at 400 kV to match the impedance of

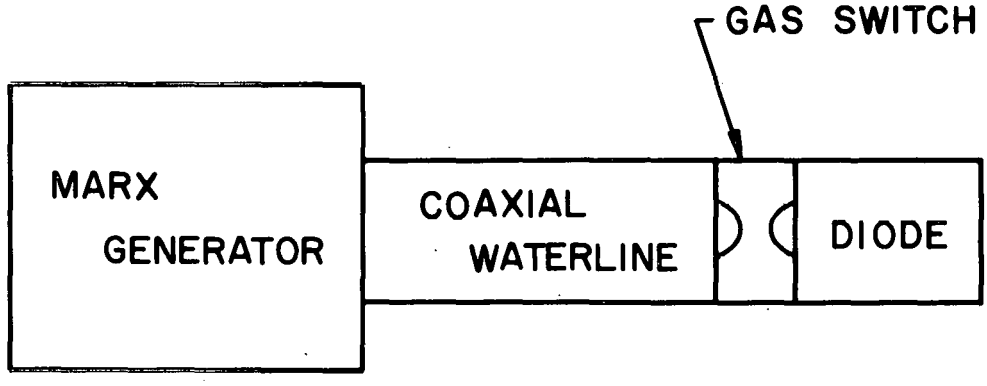

Fig. 3. Block diagram of accelerator.

the coaxial line.

The impedance of the diode in ohms is given by

$$Z = \frac{136\pi}{V_d^{\frac{1}{2}}} \frac{d^2}{A} \qquad (1)$$

where

d = anode-cathode spacing

V_d = diode voltage in megavolts

A = area of beam at the anode .

The cathode dimensions of 1.3 cm x 24.3 cm gives the required current density. The cathode emitter consists of five "saw blades," the teeth of which provide multiple emitting surfaces. The total area of the beam at the anode was originally designed to be approximately 70 cm^2 (2.5 cm x 27.3 cm). The anode-cathode spacing was then calculated to be 1.25 cm. Measurements of the electron-beam uniformity were made at the anode by exposing bleachable cinemoid film[5] to the electron beam. Anode-cathode gap spacings of 1.02 cm and 1.52 cm were used at various Marx charge voltages. The 1.52 cm spacing appeared to give the most uniform emission and, therefore, was used for the rest of the study. The charge voltage, diode voltage, diode current, measured impedance and calculated impedance are given in the following table.

Marx Charge Voltage (kV)	V_d(kV)	I_d(kA)	Z Measured (Ω)	Z Calculated (Ω)
30	390	28	13.9	23.1
34	437	34	12.8	21.9
36	475	38	12.5	21.0
38	519	40	13.0	20.1

As can be seen from the latter two columns of the table, there is a very large discrepancy between measured and calculated impedance. The disagreement could be due to the fact that the area of the beam at the anode is larger than 70 $cm.^2$ If the area were ≈ 110 cm^2, then the measured and calculated impedance would be in fair agreement. A larger area would also explain the large discrepancy between the diode energy and the energy measured by the calorimeter. These discrepancies will be addressed in a later section.

IV. Design and Construction of the Laser Cell

A laser cell was needed that had the smallest unexcited volume as possible. This was accomplished by constructing the laser cavity with a square cross section and using the anode foil and a burst diaphragm to make up two of the cavity sides. This is shown in Fig. 1. The only unexcited volume in the laser cell is that associated with the vacuum and probe ports and a small dead volume adjacent to each window. The total cavity volume is 0.531 ℓ, of which 0.234 ℓ is excited by the electron beam. A complete set of laser cavity drawings is located in the appendix at the end of this report.

There are three sets of viewing ports vertically through the cell with sapphire windows. For some experiments a cw HF probe laser is passed through these ports and the laser cavity. One port has been modified for the insertion of a pressure gauge. There are also small pressure probe tubes that allow pressure measurements at the anode.

Provisions were made inside the cell to install partitions that isolate a volume of 16.38 cm^3 (1 in^3), located in the center of the cell. This feature allows experiments to be performed on an small, known volume.

As shown in Dwg. 4, unwanted light reflection inside the laser cavity has been suppressed by machining small v-grooves perpendicular to the optical axis on all inside surfaces, except the vacuum and probe holes. In addition, the

output windows are constructed of 0.64 cm thick sapphire and are inclined 20^{o} to the laser axis so as to prevent reflections into active laser volume and thereby reducing the possibility of parasitic laser modes.

The hibachi shown in Fig. 1 and in Dwg. 3 is used to support the anode foil against the overpressure resulting from F_2, O_2, and H_2 ignition. The hibachi open area is 89% of the anode area. The construction of the burst diaphragm holder is shown in Dwg. 6 and is supported similarly to the the anode holder, except the rib support spacing is wider. This wider rib spacing provides less support to the foil and allows the burst diaphragm to rupture at a lower overpressure than that necessary to break the anode foil. This then relieves the cell pressure which prevents the anode foil from rupturing. The burst diaphragm also allows HF gas which is produced during the chemical reaction to be removed quickly from the cell to prevent etching of the windows.

V. Design and Construction of Electron-Beam Calorimeter

In order to measure the electron-beam profile and to determine the energy entering the laser cell, a "totally-stopping" calorimeter was designed and constructed. Most totally-stopping calorimeters used in the past were made from carbon. However, since carbon and a number of other materials react with fluorine, new materials were employed for the present calorimeter. The segmented elements of the calorimeter were made of aluminum and were thicker than the range of a 700 kV electron. The material used to insulate the elements were also fluorine compatible. Thus constructed, this was the first capable of measuring electron loss in a fluorine atmosphere.

A photograph of the calorimeter is shown in Fig. 4. Each of the 48 segmented elements is 2.34 cm x 0.56 cm x 0.25 cm thick. Chromel-Constantan thermocouples are mechanically attached to each element. The specific heat for Al is 0.214 cal/gm^{o}C, the weight of each element is 0.85 gm and the thermocouple constant is 0.063 mV/^{o}C.

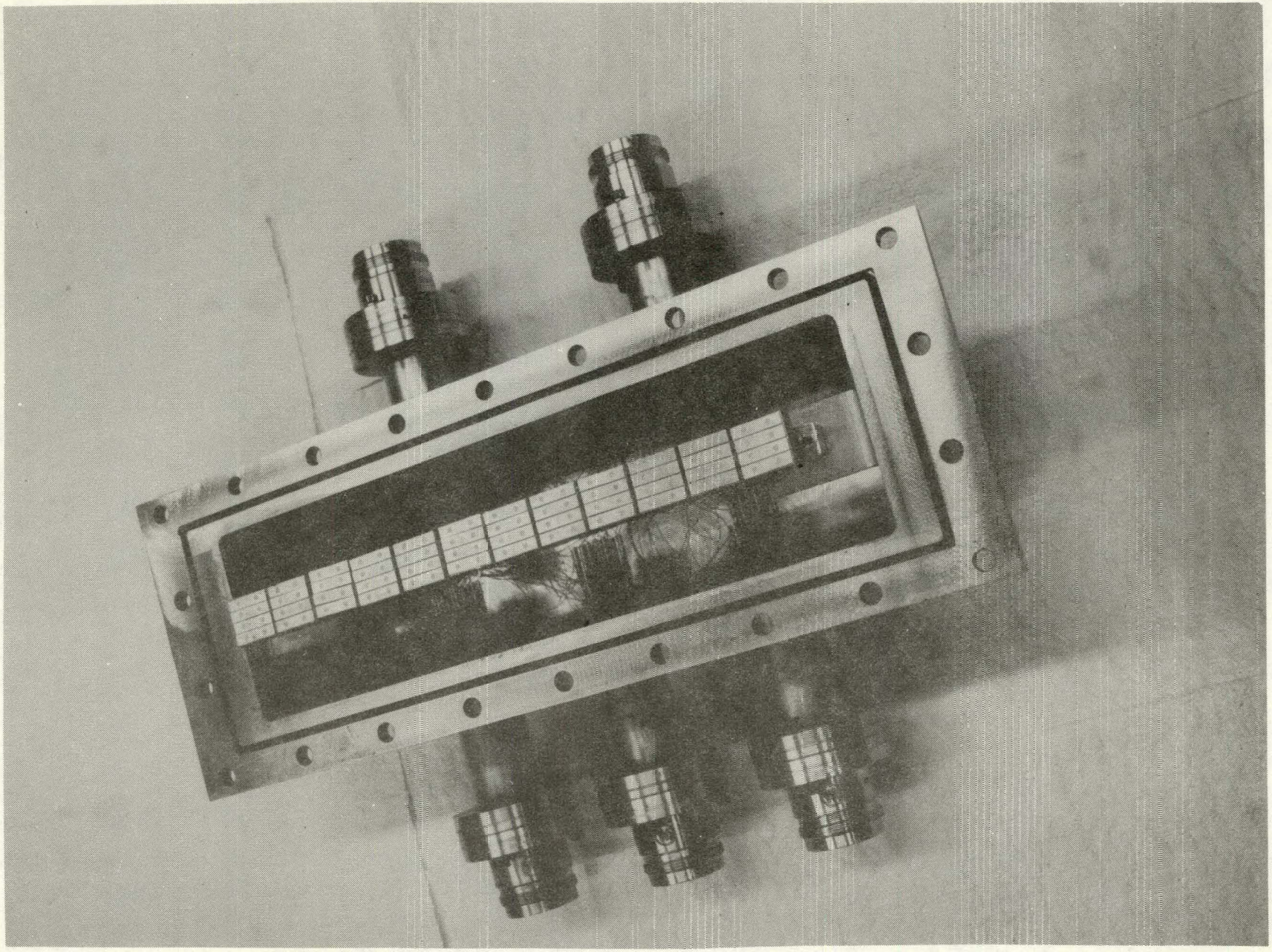

Fig. 4. Photograph of segmented calorimeter.

Therefore, the sensitivity of each element of the calorimeter is:

$$\frac{0.214 \frac{cal}{gm°C} \times 0.85 \text{ gm} \times 4.186 \frac{J}{cal}}{0.063 \frac{mV}{°C}} = 12.086 \frac{J}{mV}$$

The output voltage of each of the elements is recorded on a strip-chart recorder. It was originally envisioned that the calorimeter would be used to determine the deposited energy; however, because of the short electron-beam path length (2.5 cm) and relatively low pressure used, the amount of the electron-beam energy deposited in the gas was only a few percent of the total energy. This made the measurements difficult, and it was therefore decided to use the calorimeter mainly for uniformity measurements and to use an alternate pressure rise technique to obtain deposited energy.

VI. Measurements

A. Accelerator Measurements

Initial measurements on the device provided operating characteristics of the machine and a rough estimate of beam uniformity as a function of anode-cathode spacing. A few important machine operating charactersitics measured were: self-breakdown voltage versus pressure for both the spark-gap switches in the Marx and the main switch. The self-breakdown versus pressure curves were very similar to those given in the machine instruction book; therefore, they will not be duplicated here. Diode characteristics were determined at charge voltages of 30, 34, 36 and 38 kV. The diode energy $\int VIdt \approx V_{max} I_{max} T_{FWHM}$ as a function of diode voltage is shown in Fig. 5, which indicates a maximum diode energy of 1045 J at a diode voltage of 518 kV (38 kV charge). The actual energy which was measured by the calorimeter placed at the anode under these conditions was 320 J which means that nearly 70% of the energy did not enter the laser cell. It is suspected that much of the energy loss in the hibachi; however, some of this energy loss was simply due to the fact that the beam at the anode surface

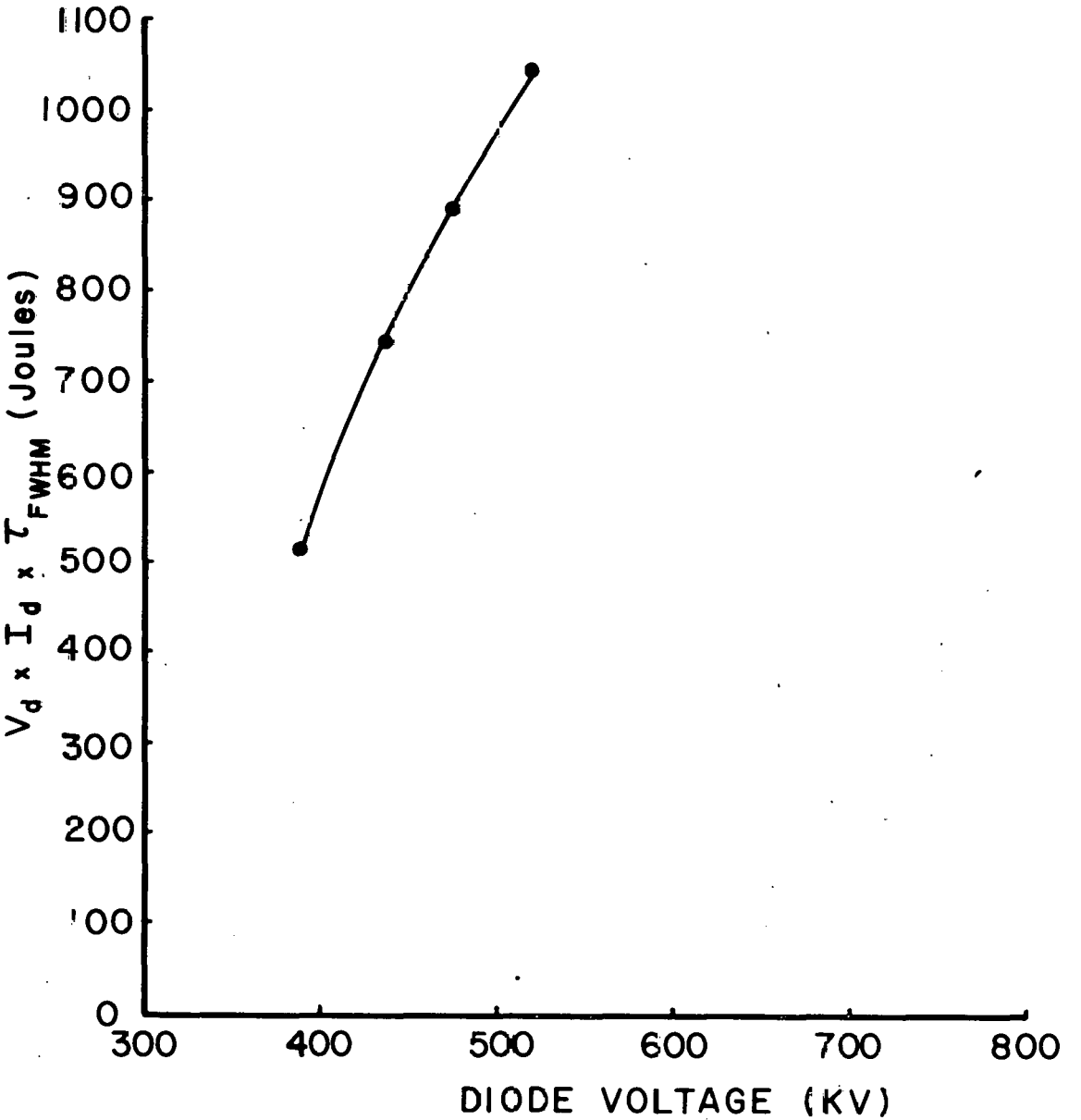

Fig. 5. Diode energy as a function of diode voltages.

was larger than the opening to the laser cell.

B. Calorimeter Measurements

The calorimeter system was used to measure the electron-beam distribution near the anode and to obtain the energy deposition in high pressure SF_6. In this case, the amount of energy deposited in the gas is a large fraction of the energy passing through the foil. Figure 6 shows the electron-beam distribution at a distance of 0.16 cm from the anode. The overall dimensions of the calorimeter are 2.54 cm by 29.0 cm. The area of the cathode shown in Fig. 1 and in Dwg. 8 is 1.3 cm by 24.3 cm. As shown by Fig. 6, the distribution is peaked in the center, which corresponds to the peak emission area of the cathode. The uniformity across the cell varies by about a factor of two, which is not as good as anticipated, but is sufficient for the initial measurements. The total energy through a 0.001-inch stainless steel anode foil was 319 J for a diode voltage of 518 kV.

Figure 7 shows three electron-beam profiles, taken at the farthest possible distance of 2.29 cm (0.9 inches) from the anode. These profile measurements were taken while using an anode foil of 0.003 inch-thick stainless steel, thereby causing a considerable amount of energy ($\approx$30%) to be deposited in the foil. This thick foil was necessary to hold the pressure ($\approx$3000 Torr) needed for these experiments. The total energy measured at 3 Torr of SF_6 at a distance of 2.29 cm was 168 J, while that at the anode foil was 230 J. This indicates that approximately half of the energy was scattered out of the cell, because the fraction represented by absorption in the gas is negligible at 3 Torr of SF_6. The profiles shown in Fig. 7 are much more uniform away from the anode than at the anode which indicates a lot of scattering since scattering tends to make the distribution more uniform. The lower two distributions shown in Fig. 7 give the energy absorbed by the calorimeter when 3000 Torr of SF_6 is present in the cell.

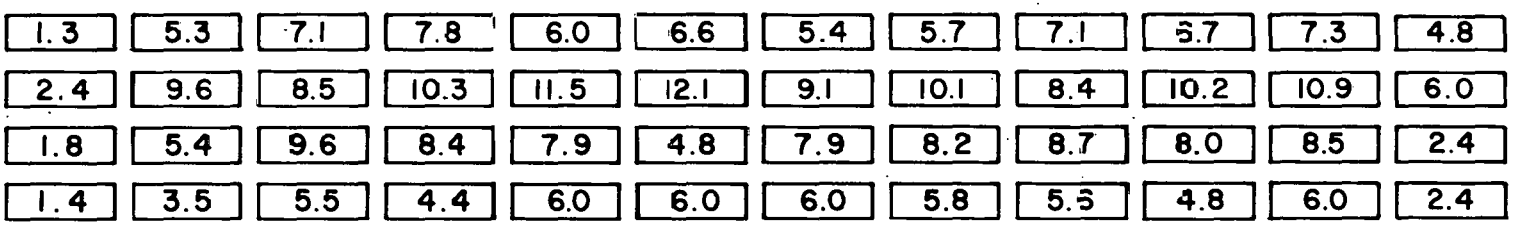

Fig. 6. Electron-beam distribution near the anode.

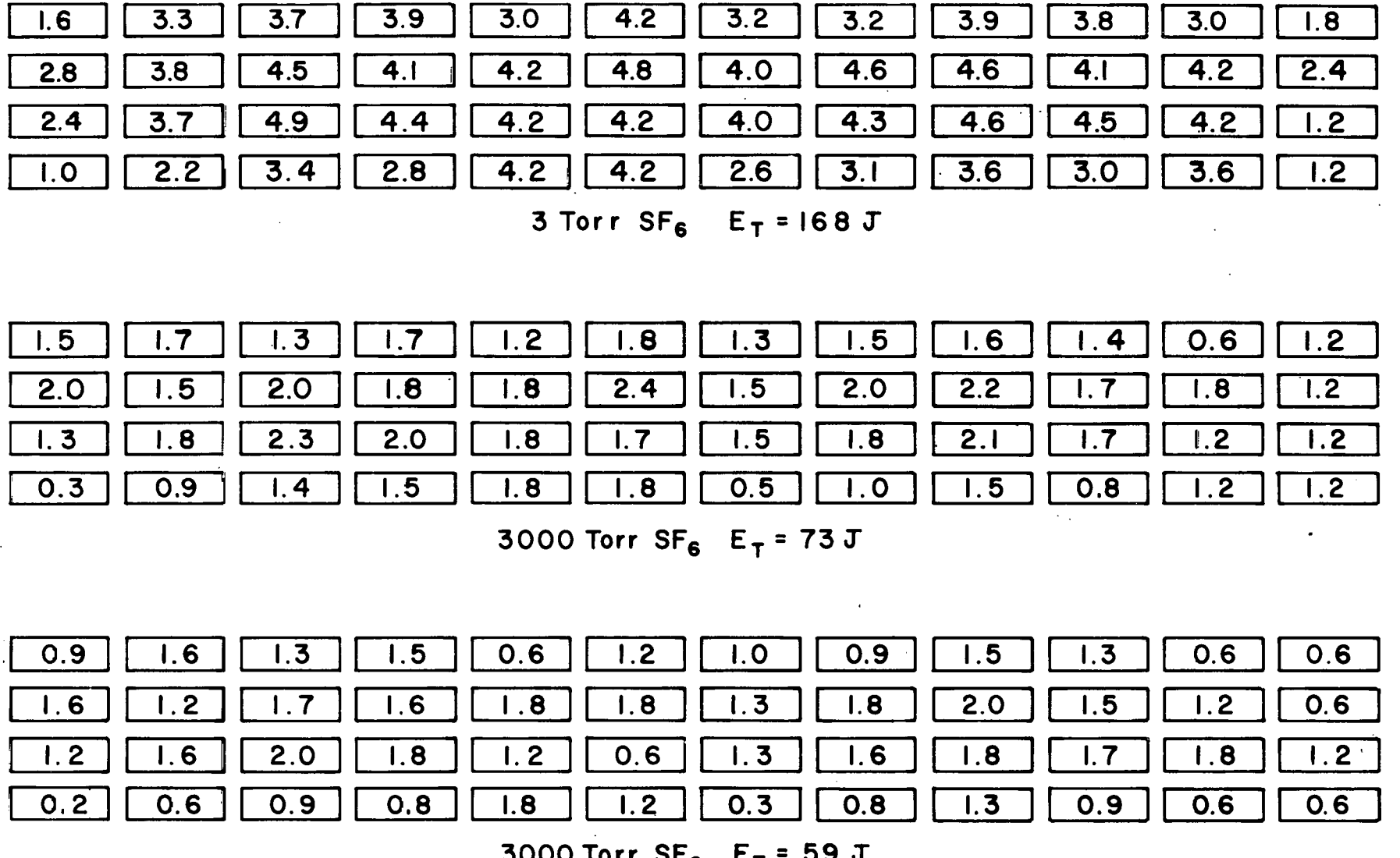

Fig. 7. Electron-beam distribution in SF_6 at a distance of 2.29 cm from anode.

Here again the distributions are more or less uniform away from the anode. The difference in the transmitted energy at the anode at 3000 Torr (73 J and 59 J) represent the accuracy of the measurements and the reproducibility of the electron-beam machine. The difference between the transmitted energy using 3 Torr SF_6 and 3000 Torr SF_6 gives an upper bound for the energy deposited in the 3000 Torr SF_6. These values of 95 and 109 J obtained by calorimetry will be compared to the pressure rise measurements explained in the next section.

C. Pressure Rise Measurements

In order to determine the energy deposited in the cell at lower pressures, a pressure rise technique was used. If energy is added to an ideal gas of a constant volume (V), the temperature (T) will rise according to PV = NRT. The pressure rise is given by T/T = P/P. Since the energy deposited is related to the change in temperature by $E_{dep} = C_v \Delta T$, then

$$E_{dep} = C_v T(°K) \frac{\Delta P}{P} \frac{cal}{gm} \qquad (2)$$

where C_v is the specific heat at constant volume, T is the temperature in degrees kelvin, P is the initial pressure and ΔP is the measured pressure rise. Equation (2) will be valid whenever processes like radiation are not important. Comparisons of the deposited energy by this pressure rise technique and with total stopping calorimeters have been made on the λ-3 device.[6] Good agreement was obtained for N_2; however, the pressure rise measurements for argon, which radiates up to 40% of its energy, gave deposition values smaller than those obtained by argon deposition scaled from N_2. In general, the pressure rise measurements are made in nitrogen and results for other gases are scaled according to density.

The pressure rise is measured for the entire volume including the excited

and unexcited regions. In order to determine the energy density deposited in the excited region alone, Eq. (2) should be multiplied by the ratio of the unexcited to excited volume. In our case, 0.531 ℓ/0.234 ℓ. One must use this value to determine energy expended per F atom, which will be discussed later.

Pressure-rise measurements were performed in nitrogen at a variety of diode voltages and in other gases (F_2 and SF_6) at the maximum diode voltage of 518 kV. Figure 8 shows P as a function of pressure for four different Marx charge voltages, corresponding to diode voltages of 390 kV, 437 kV, 475 kV and 518 kV. The data shows that ΔP is linear with pressure up to total pressures of 2400 Torr of N_2. The fact that ΔP is linear means the deposited energy at a given voltage scales with density. This should be the case if $\rho\ell$ is much less than the range of the electron where ρ is the density and ℓ is the transverse dimension of the cell. The slope of the lines in Fig. 8 is related to the energy deposited in the laser cell in joules/ℓ-atm. This value is important in chemical laser research since it determines the initiation level or the fractional amount of dissociation. This relationship is obtained from Eq. (2) and is given by

$$E_{deposited} = 0.171\ MC_V T \left(\frac{\Delta P}{P}\right) \frac{J}{\ell\text{-atm}}$$

where

M = molecular weight

C_v = specific heat at constant volume

T = temperature in ^oK.

for N_2

$$M = 28 \text{ and } C_v = 0.178 \frac{cal}{gm^oK}$$

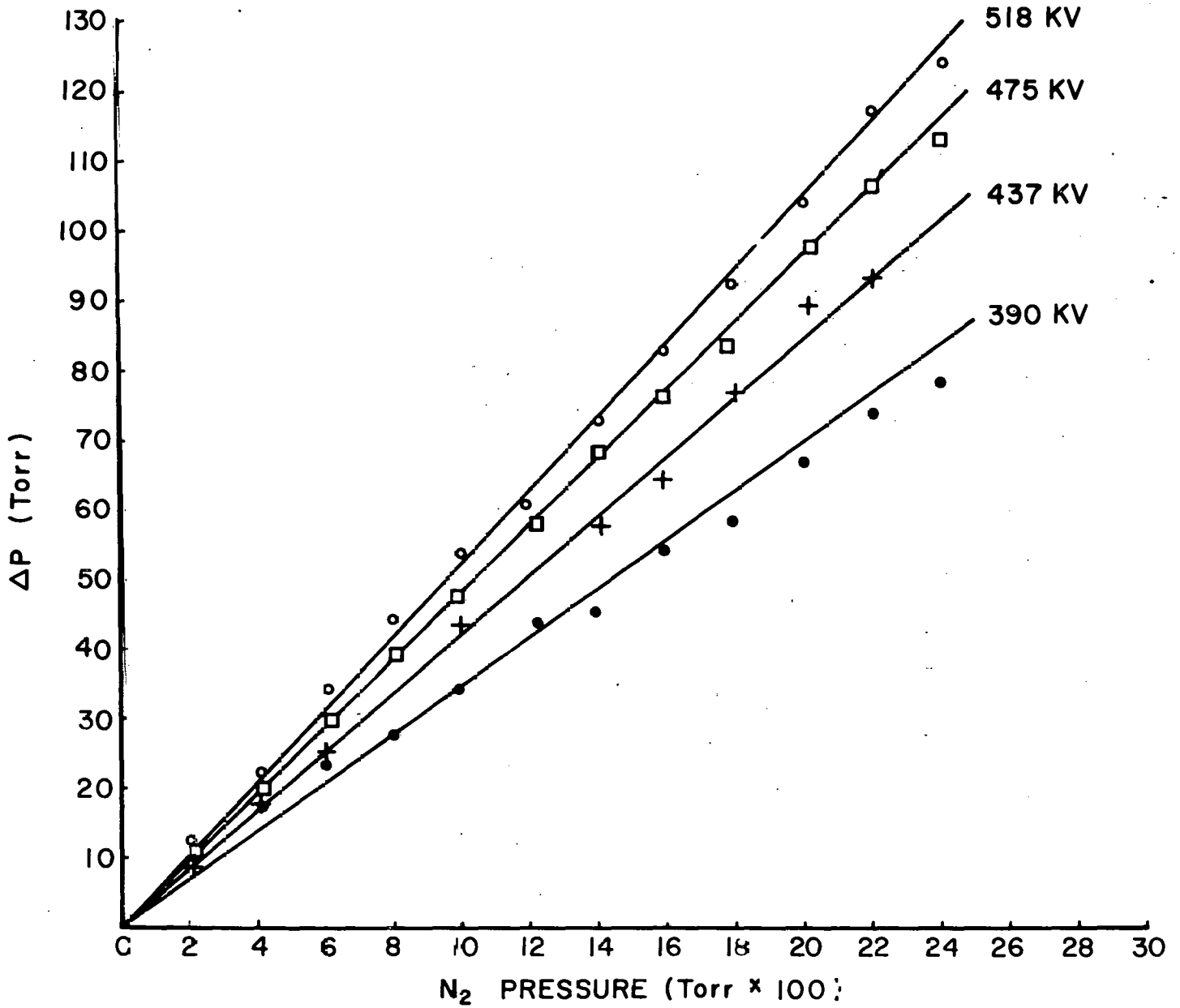

Fig. 8. Pressure rise as a function of nitrogen pressure at various diode voltages.

so

$$E_{deposited} = 255 \frac{\Delta P}{P}$$

In order for this to be useful for laser calculations, one has to multiply this by the ratio of total volume to active volume, in this case 2.29. Then $E_{deposited} = 584\ \Delta P/P$. A plot of energy deposited in J/ℓ-atm N_2 as a function of diode voltage is shown in Fig. 9. The maximum deposition level is 31 J/ℓ-atm N_2 which is similar to that of large chemical laser systems. The curve shown in Fig. 9 increases with increasing diode voltage, even though less energy would be deposited if the total energy in the diode was held constant. In our device, the total energy increased from 515 J at a diode voltage of 390 kV to 1045 J at a diode voltage of 518 kV. In other words, the input energy increased by a factor of 2.0 while the deposition only increased by a factor of 1.4.

The basic approach of the pressure rise technique is to measure the pressure rise in nitrogen (where calorimeter measurements have been shown to agree) and then density scale these results to other gases, such as argon and fluorine. In an effort to determine if the pressure rise technique could be applied to other gases, measurements were also made in F_2 and SF_6 since these are the gases of interest for chemical laser research. Figure 10 shows ΔP as a function of pressure for these three gases at a diode voltage of 518 kV. Using Eq. (3) with M = 28, $C_v = 0.178$ cal/gm^oK for N_2, M = 38, $C_v = 0.146$ cal/gm^oK for F_2 and M = 146 and $C_v = 0.145$ cal/gm^oK for SF_6, together with a volume of 0.531 ℓ, the deposition was calculated for each pressure shown in Fig. 10. In order to determine if density scaling is correct, the energy deposited is plotted against $\rho\ell$, where ρ is the density at each pressure and ℓ is the absorption length of the cell. In this case,

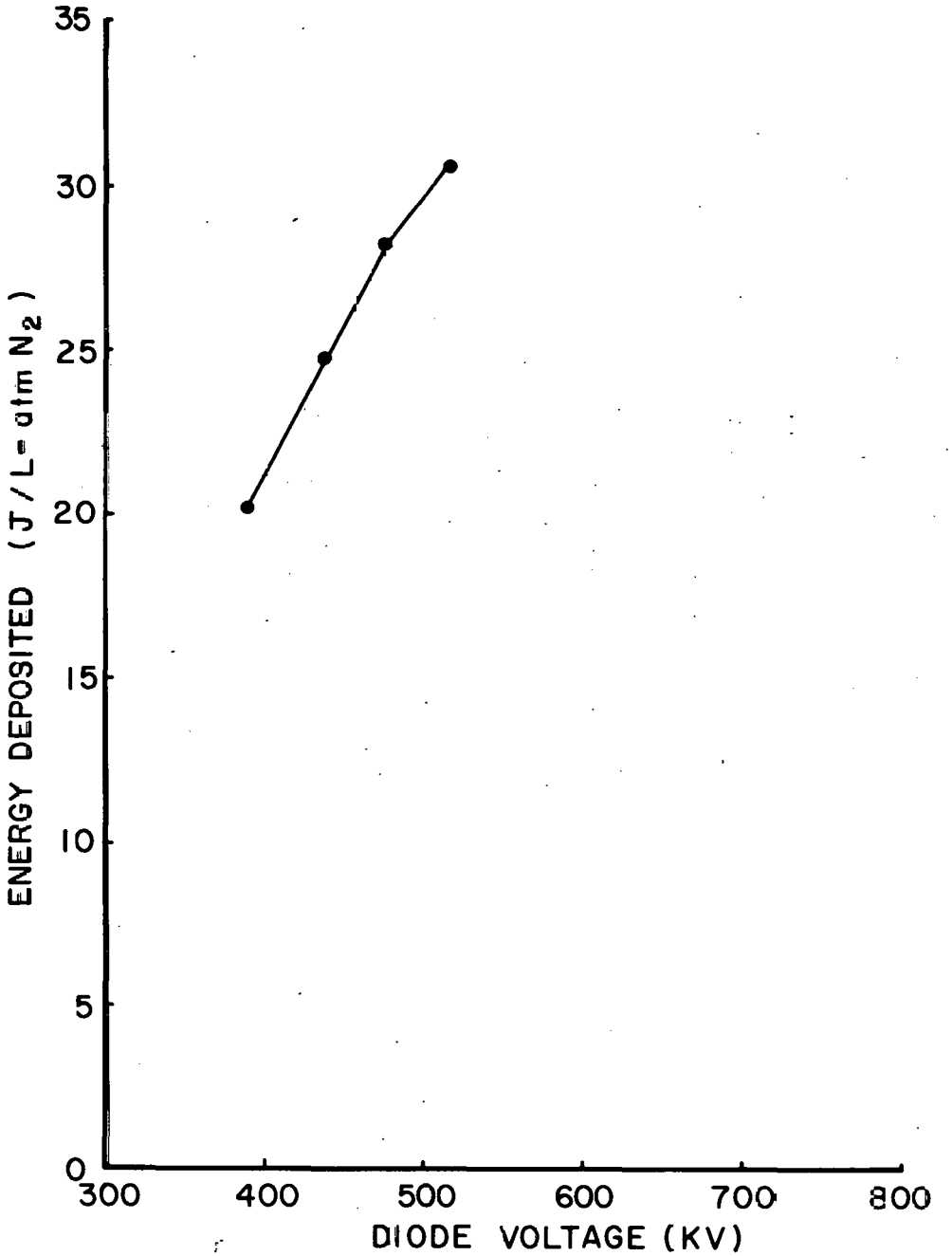

Fig. 9. Deposited energy in nitrogen as a function of diode voltage.

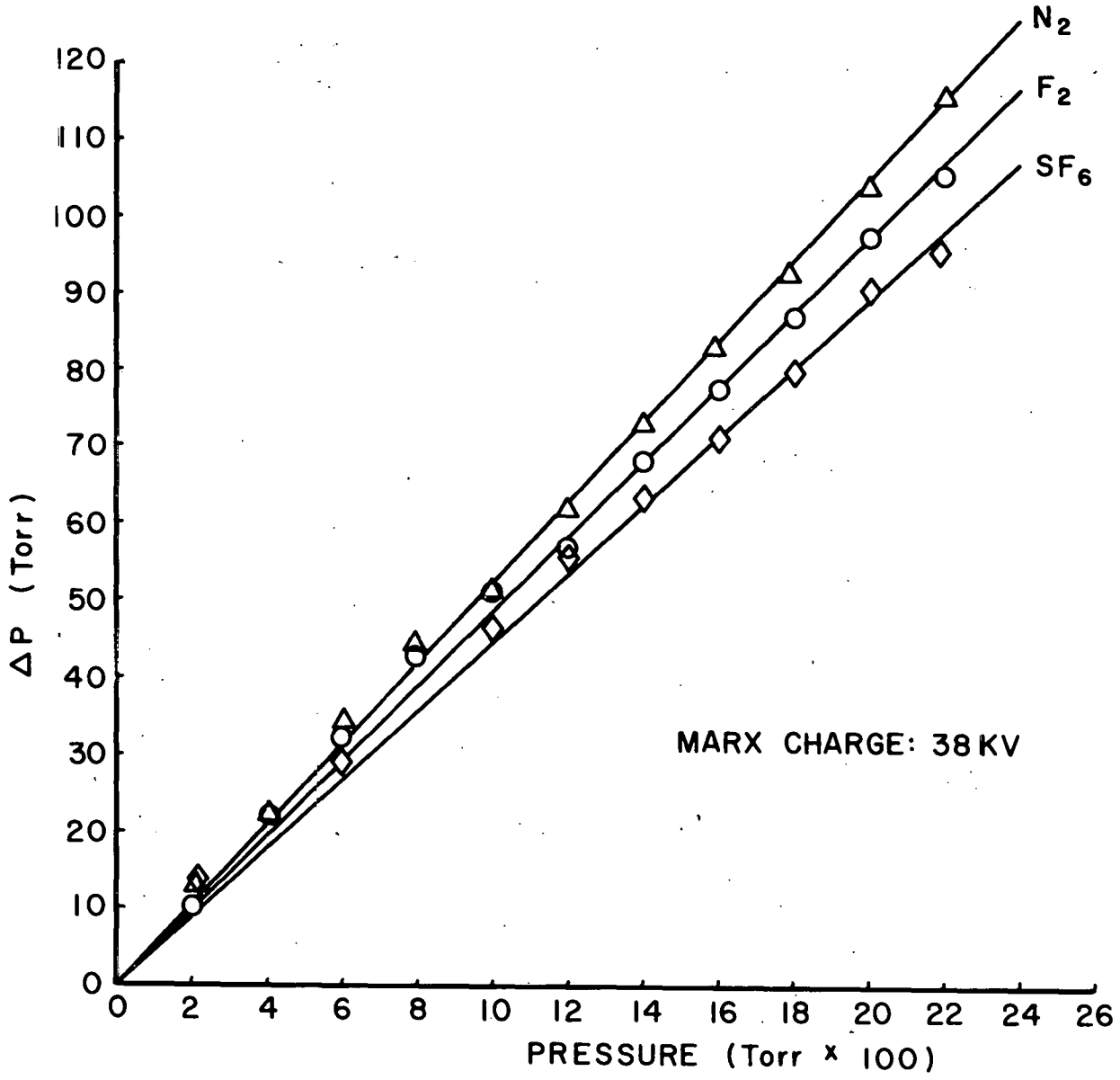

Fig. 10. Pressure rise as a function of pressure for N_2, F_2 and SF_6.

ℓ = 2.54 cm. The results, plotted in Fig. 11, show that the deposited energy as deduced by the pressure rise in F_2 and SF_6 fall below that predicted by a density scaling of N_2, shown by the dashed line. There appears to be an error of $\approx$ 50% at the highest SF_6 pressure if N_2 data is used. However, for deposition values for $0 \leq \rho\ell \leq 0.4$ where most of our laser and kinetic data were obtained, the error is insignificant. One possibility for the disagreement at high pressures is that there is a significant amount of scattering in SF_6, which was pointed out in the calorimeter studies and much of the initial energy was scattered out of the cell. The upper bound to the energy deposited at 3000 Torr SF_6 was obtained with the calorimeter system shown in Fig. 11. This measurement would suggest that the pressure rise measurement in SF_6 agrees with the calorimeter data and supports the scattering argument. It should be pointed out that a plot such as the one shown in Fig. 11 is only logical if the electron range in all the gases is similar. The range of a 500 kV electron varies from about 0.2 gm/cm^2 to $\approx$ 0.4 gm/cm^2, which is roughly a factor of 10 larger than the highest $\rho\ell$ in these studies.

The conclusion, therefore, from these pressure rise measurements is that it appears F_2, N_2 and SF_6 give roughly the same deposition values for the pressures of interest for laser studies, i.e., 100 Torr SF_6 or 500 Torr F_2, and can be scaled from N_2 measurements. The disagreement at high pressures of SF_6 can be explained by scattering since the pressure rise appears to agree with calorimeter measurements.

D. Laser Measurements

A limited number of laser shots were performed to check out the laser system. An optical cavity was formed using a flat sapphire output coupler and a totally reflecting flat copper mirror. The gas mixture for these shots was

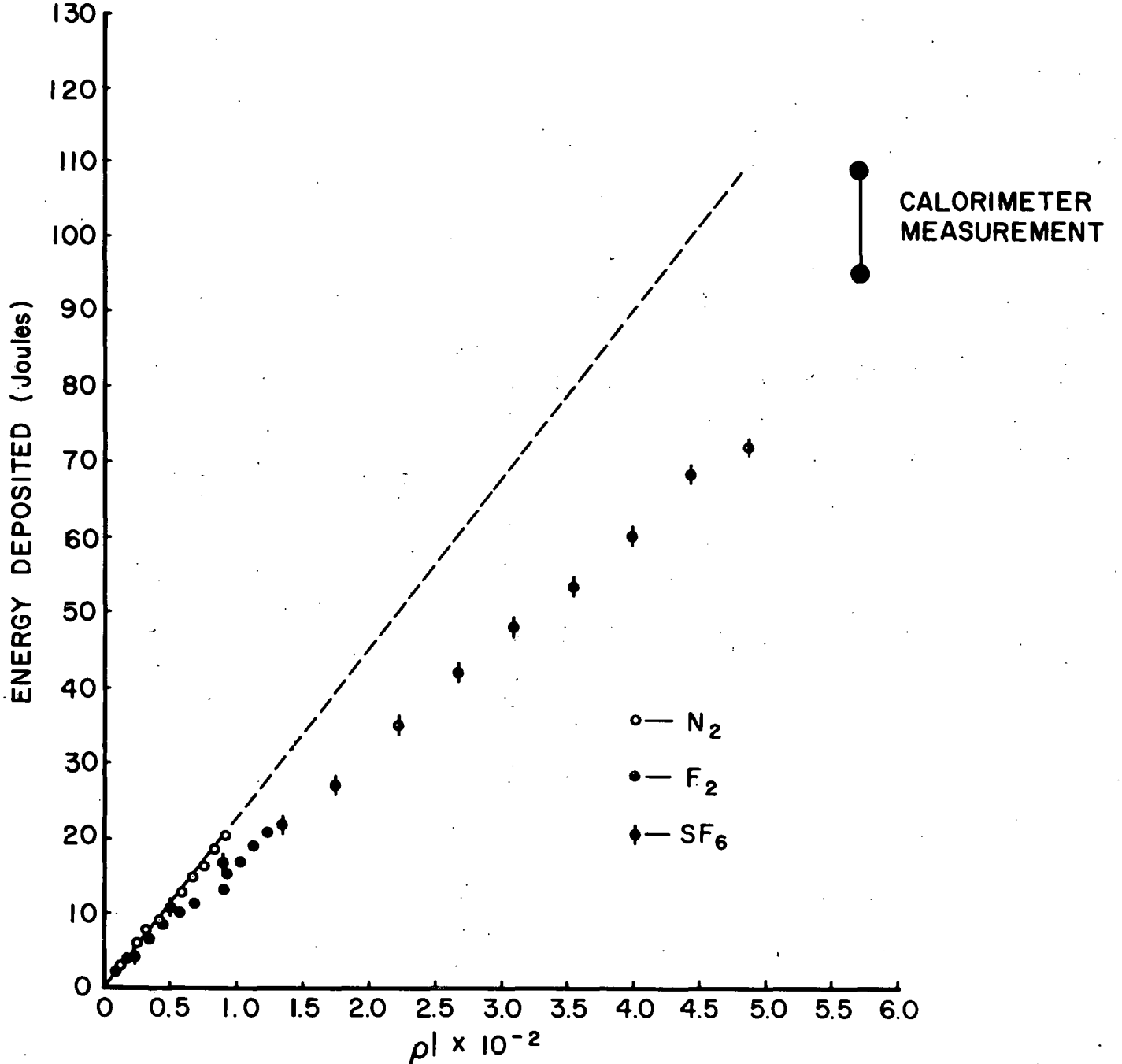

Fig. 11. Energy deposited as a function of density times length product for N_2, F_2 and SF_6.

500 Torr F_2, 150 Torr O_2 and 125 Torr H_2. Measurements included laser pulse width, laser energy and intensity distribution using "foot print" paper. The electron beam current and laser pulse time histories are shown in Fig. 12. The diode voltage for these shots was 390 kV. The laser pulse width is much longer than the electron beam pulse width as is expected using the present initiation levels. The total laser energy at this pressure and gas mixtures was 3.84 J. Using the deposition for an equivalent nitrogen pressure of 859 Torr, the energy deposited in the gas was 8.89 J, yielding an electrical efficiency of 43%, which is reasonable for HF chemical lasers. The "foot print" of the output showed that the laser medium did not have any hot spots, which also agreed with our uniformity measurements.

E. Other Measurements

The apparatus was also used to measure the optical absorption of the $P_1(7)$ line of HF as a function of HF pressure in order to compare with previous measurements. The energy expended per fluorine atom in SF_6-$H_2(C_2H_6)(HC\ell)$ gas mixtures was also determined. This experiment involved measuring the amount of HF produced when the electron beam excited these mixtures. The results of these two series of experiments will be published in the near future.

VII. Conclusions

The T-3 laser system, designed for HF/DF chemical laser studies, is described herein. The system performance was outlined with particular attention paid to beam uniformity and energy deposition. The diagnostics for measuring the system performance were chiefly calorimetry and pressure rise experiments, both of which were discussed in detail. Finally, some HF laser experiments done with the T-3 system are briefly outlined along with their results.

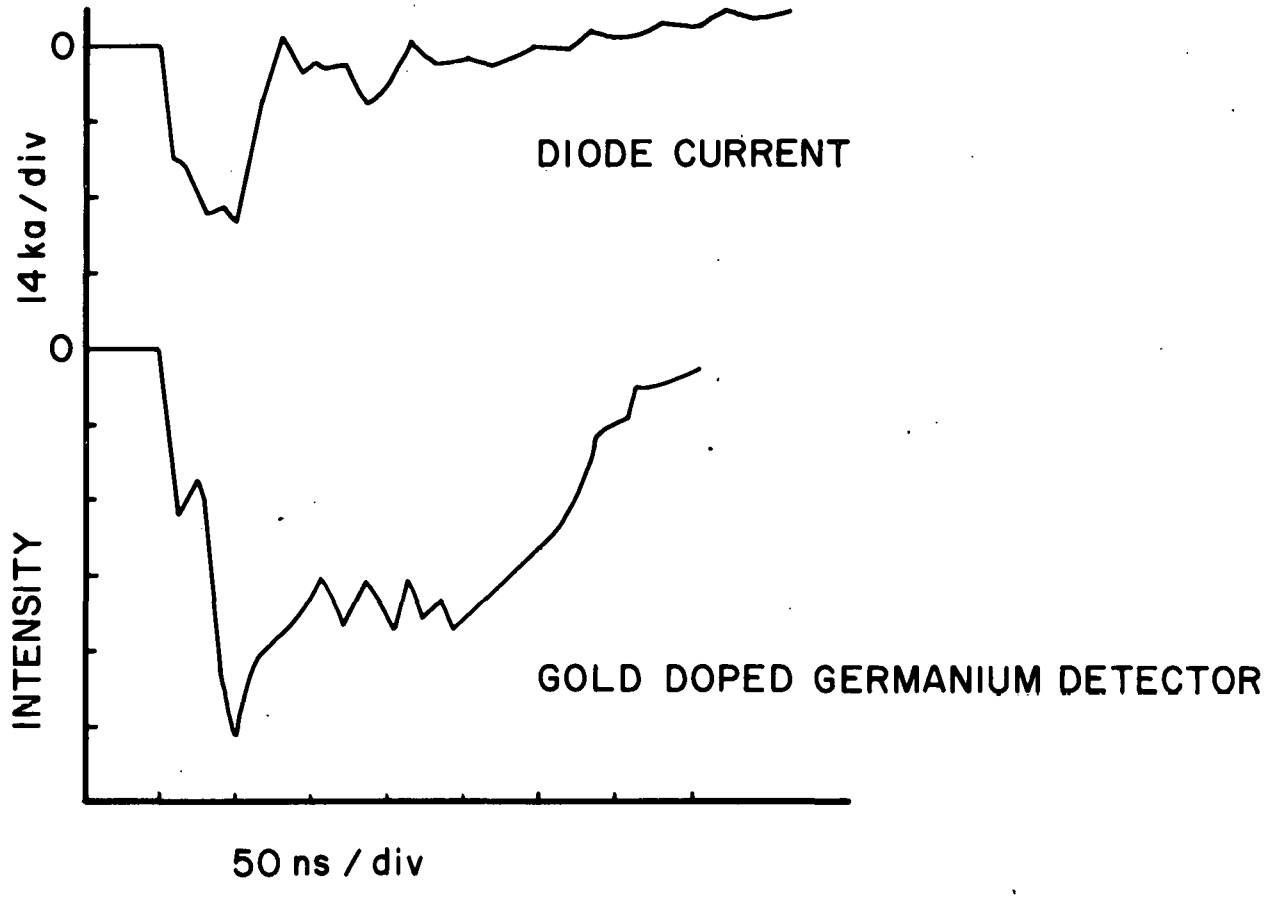

Fig. 12. Electron-beam current and laser intensity time histories.

REFERENCES

1. Physics International Company, San Leandro, CA, PI Report No. PIMM 893.
2. A. K. Hays, J. M. Hoffman, and G. C. Tisone, "Development of A Pulse-Per-Second KrF Laser," SAND76-0422, Sandia National Laboratories, Albuquerque, NM, November 1976.
3. R. A. Klein, "Gas Handling System for Sandia HF Laser Facility," Internal Memorandum, Sandia National Laboratories, Albuquerque, NM 87185, March 1979.
4. Physics International, San Leandro, CA, TG-70 Pulse Generator.
5. Cinemoid, Holtzmueller Corporation, 2545 16th Street, San Francisco, CA 94103.
6. G. C. Tisone and E. L. Patterson, private communication.

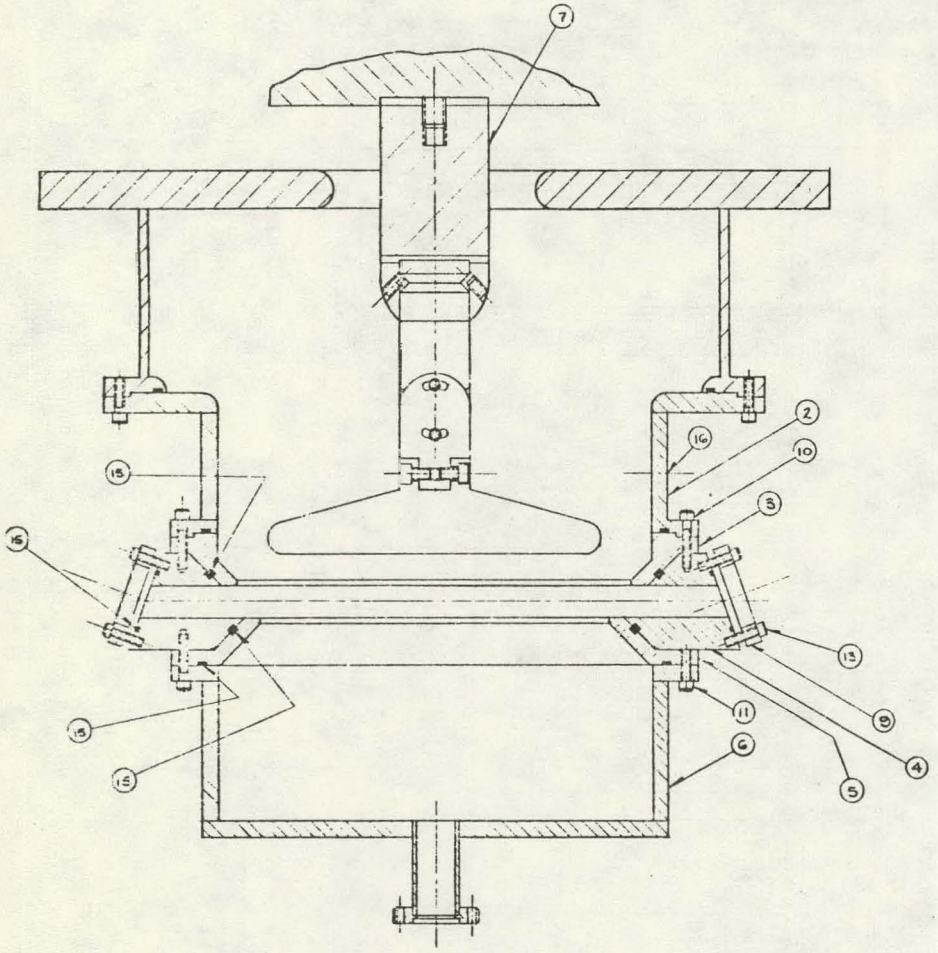

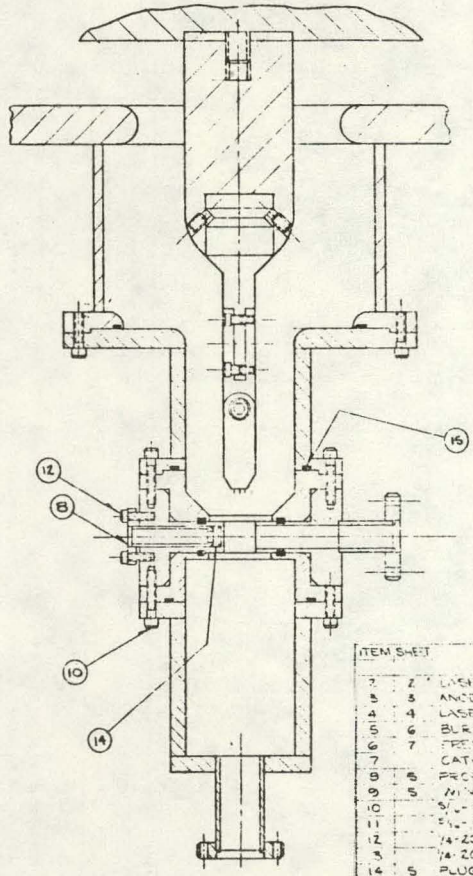

ITEM	SHEET	DESCRIPTION	QTY
2	2	LASER CELL ADAPTER	1
3	3	ANGLE HOLDER	1
4	4	LASER CAVITY	1
5	6	BURST DIAPHRAGM HOLDER	1
6	7	PRESSURE RELIEF TANK	1
7		CATHODE ASSEMBLY - SEE T6 0206	1
8	8	PROBE WINDOW HOLDER	1
9	5	WINDOW RETAINER	2
10		5/16-18NC-2 x 1 3/8 LONG HEX HD CAP SCR. STEEL	4
11		5/16-18NC-2 x 3/4 LONG HEX HD CAP SCR. STEEL	6
12		1/4-20NC-2 x 3/8 LONG SOC HD CAP SCR. STEEL	2
13		1/4-20NC-2 x 1 LONG SOC HD CAP SCR. STEEL	12
14	5	PLUG	6
15		O-RING 1/8 DIA. AS REQ'D. VITON	
16		1/4-18NPT PIPE PLUG	3
17			
18			
19			
20			
21			
22			
23			

Dwg. 1. Laser Cavity Assembly (PPS)

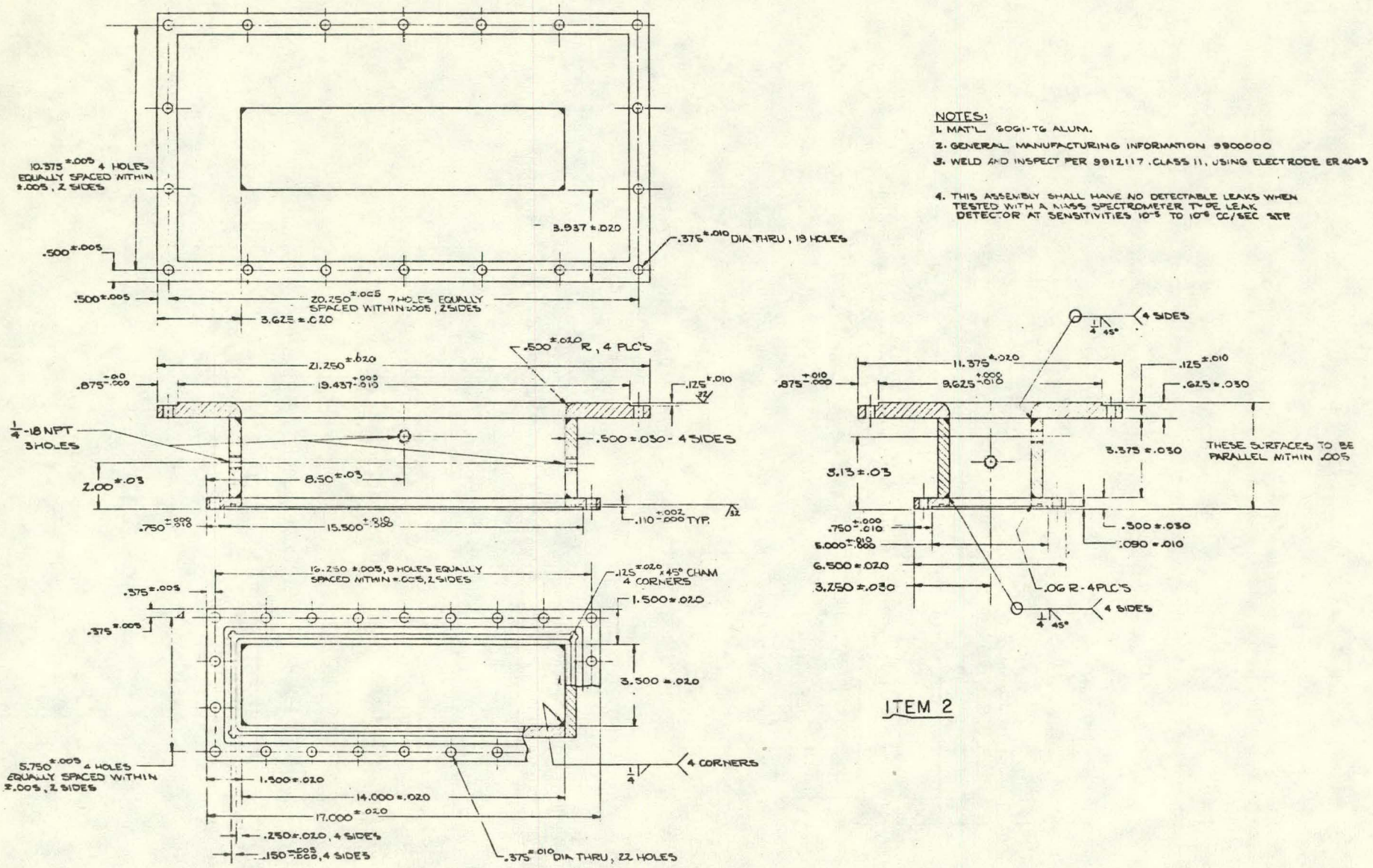

ITEM 2

Dwg. 2. Laser Cell Adapter (PPS)

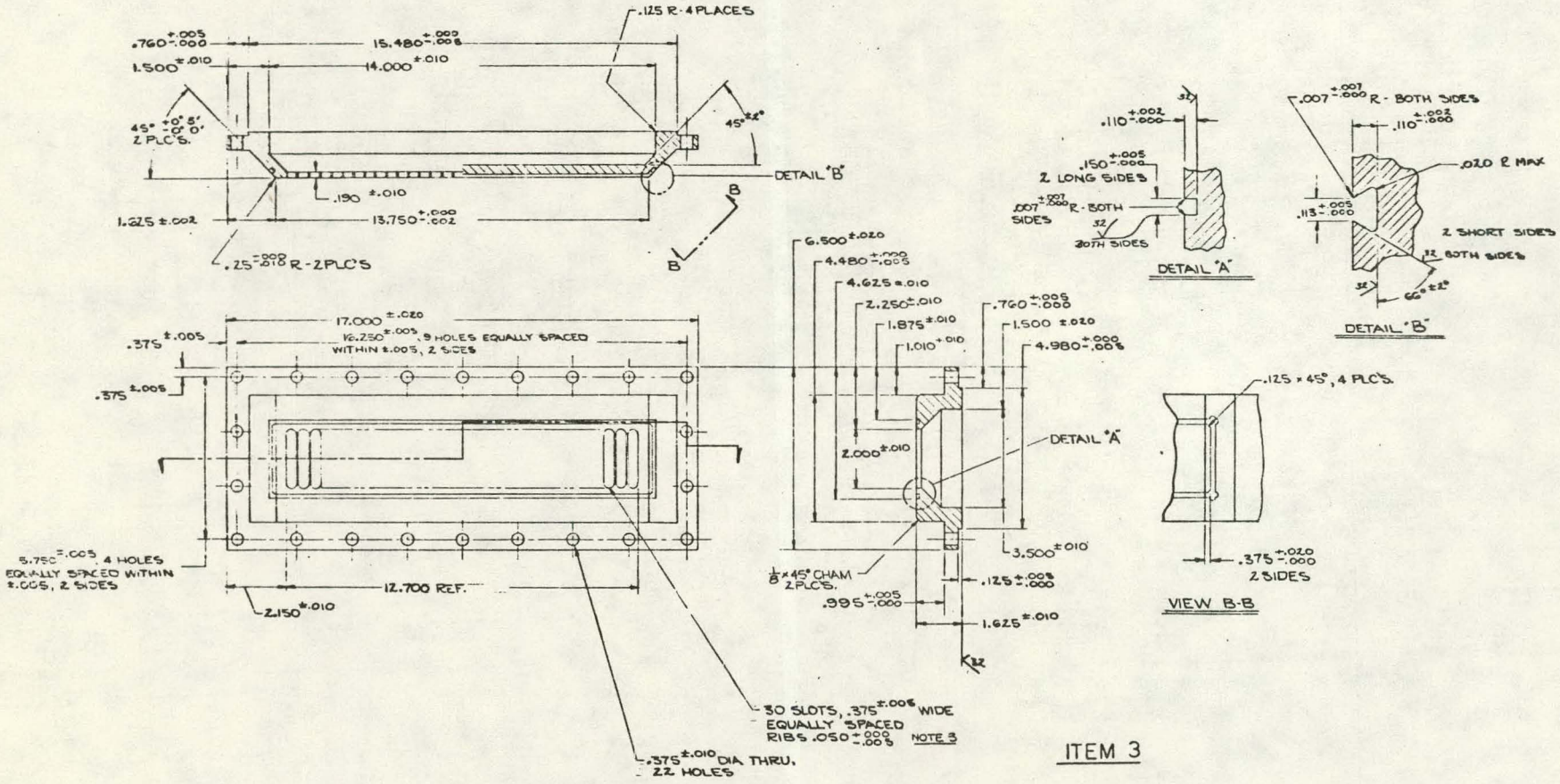

Dwg. 3. Laser Cavity Anode Holder (PPS).

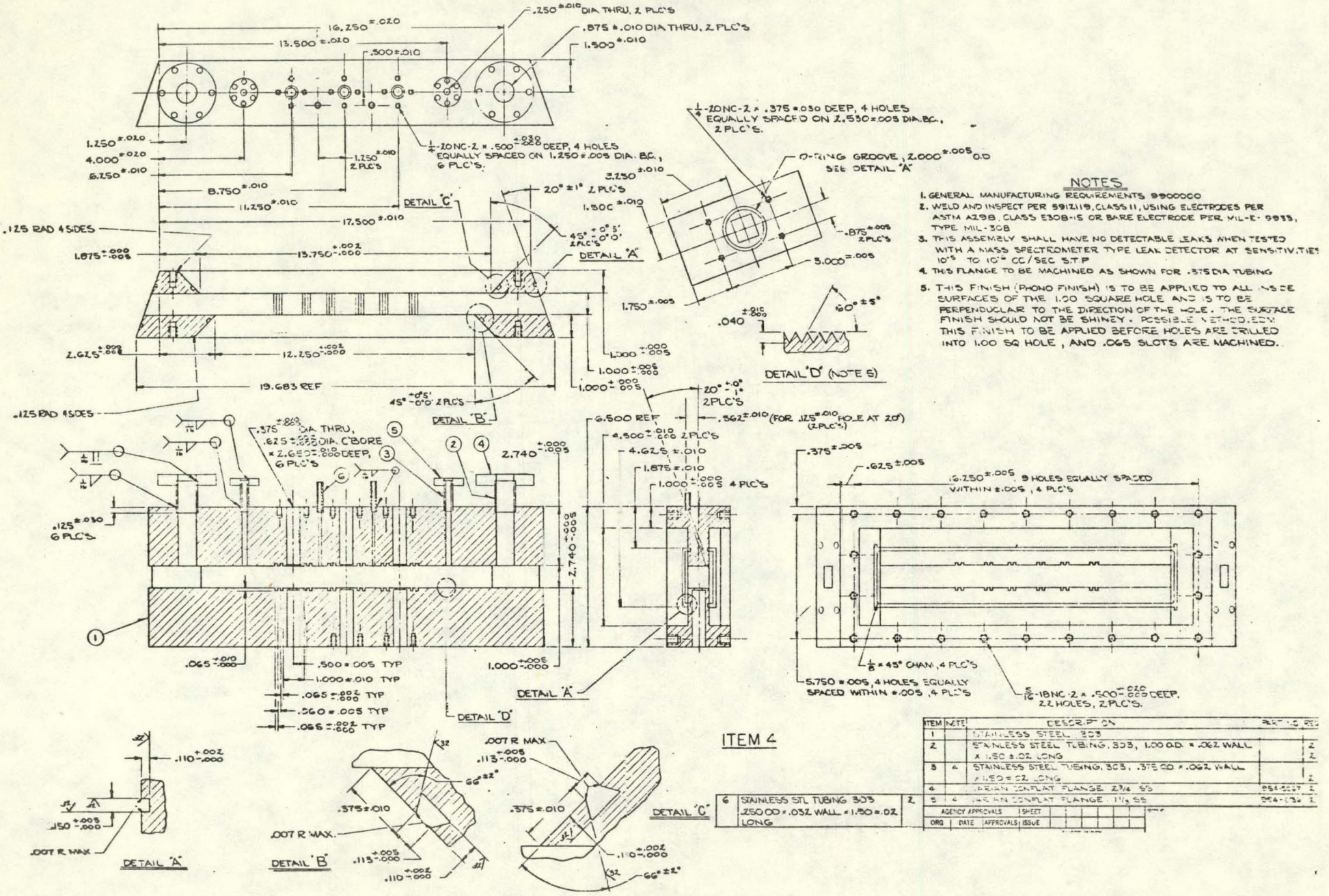

ITEM	NOTE	DESCRIPTION	REQ'D
1		STAINLESS STEEL 303	
2		STAINLESS STEEL TUBING, 303, 1.00 O.D. × .062 WALL × 1.50 ± .02 LONG	2
3	4	STAINLESS STEEL TUBING, 303, .375 OD × .062 WALL × 1.50 ± .02 LONG	2
4		VARIAN CONFLAT FLANGE 2 3/4 SS	954-5007 2
5	4	VARIAN CONFLAT FLANGE 1 1/3 SS	954-5034 2
6		STAINLESS STL TUBING 303 .250 OD × .032 WALL × 1.50 ± .02 LONG	2

AGENCY APPROVALS		SHEET
ORG	DATE	APPROVALS	ISSUE

Dwg. 4. Laser Cavity (PPS)

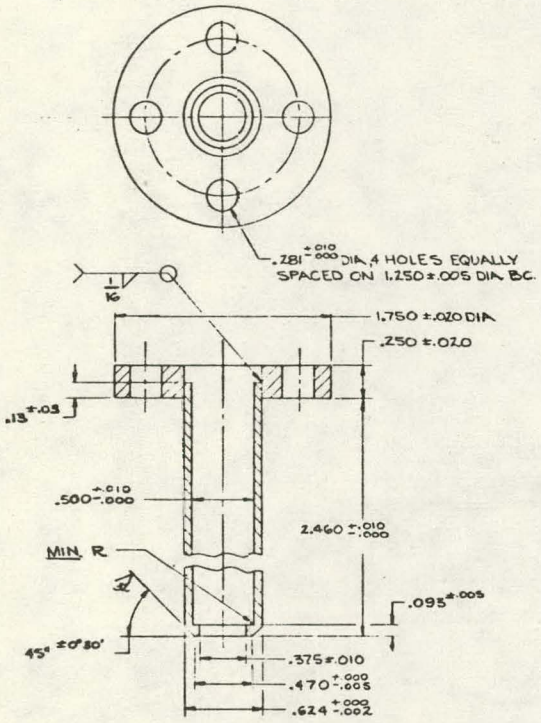

PROBE WINDOW HOLDER
MAT'L: 303 STAINLESS STL.
6 REQ'D

ITEM 8

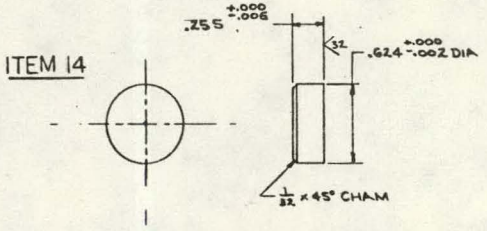

ITEM 14

PLUG
MAT'L: 304 STAINLESS STL.
6 REQ'D

NOTES
1. GENERAL MANUFACTURING INFORMATION 9900000

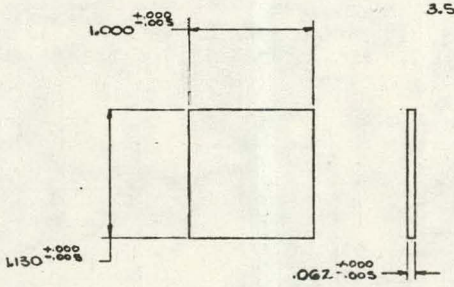

BAFFLE
MATL. 303 STAINLESS STL.
12 REQ'D

ITEM 17

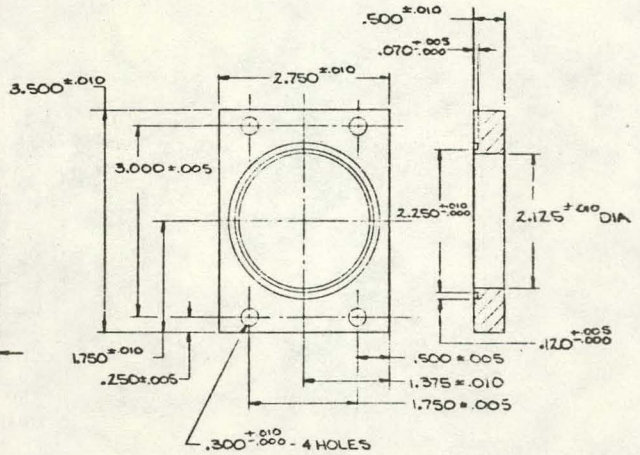

WINDOW RETAINER
303 STAINLESS STL.
2 REQ'D

ITEM 9

Dwg. 5. Laser Cavity (PPS)

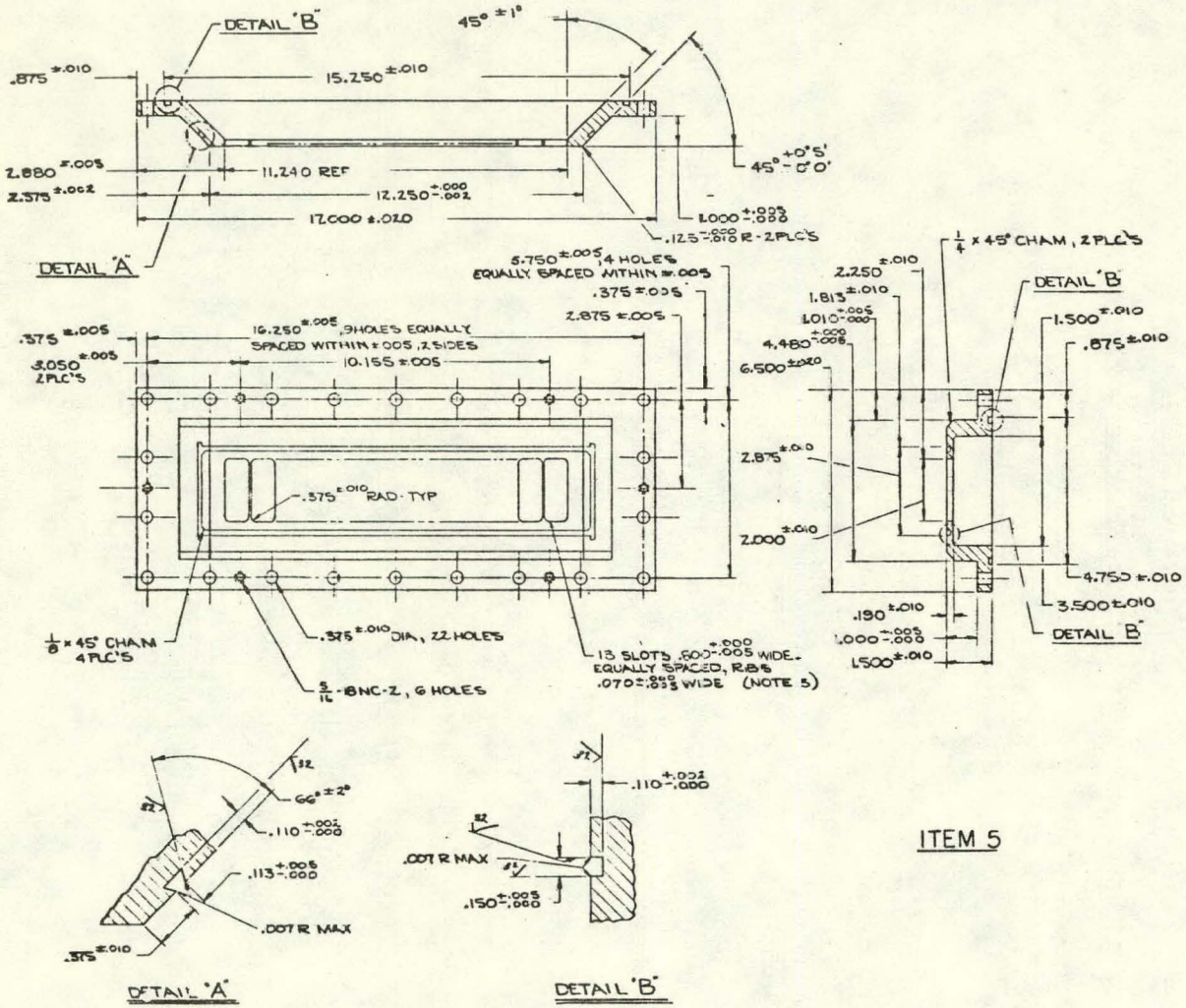

ITEM 5

NOTES

1. GENERAL MANUFACTURING INFORMATION 8900000
2. MAT'L: 303 STAINLESS STEEL
3. BREAK ALL EDGES AROUND SLOTS .005

Dwg. 6. Laser Cavity Burst Diaphram Holder (FPS)

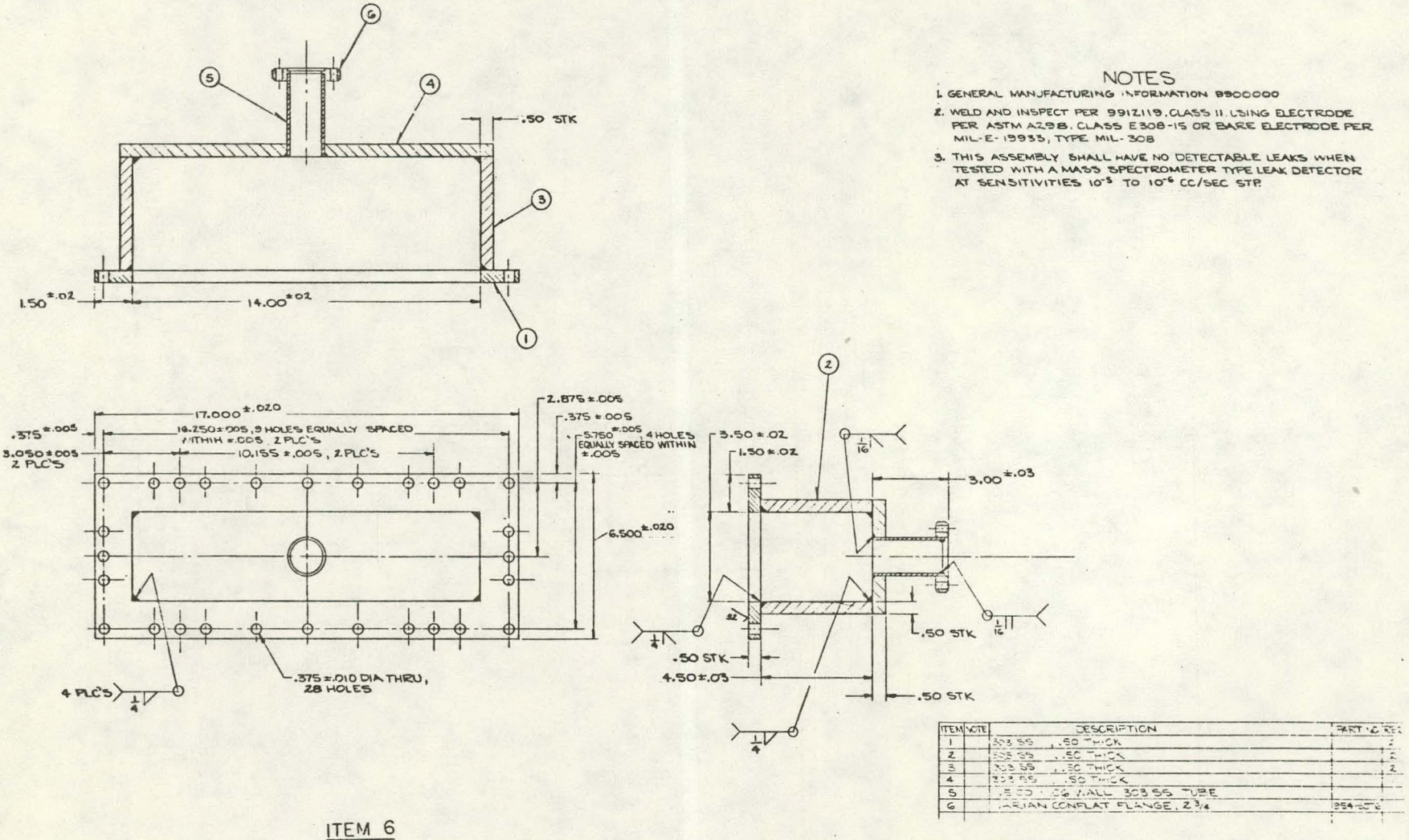

ITEM 6

Dwg. 7. Laser Cavity Pressure Relief Tank (PPS)

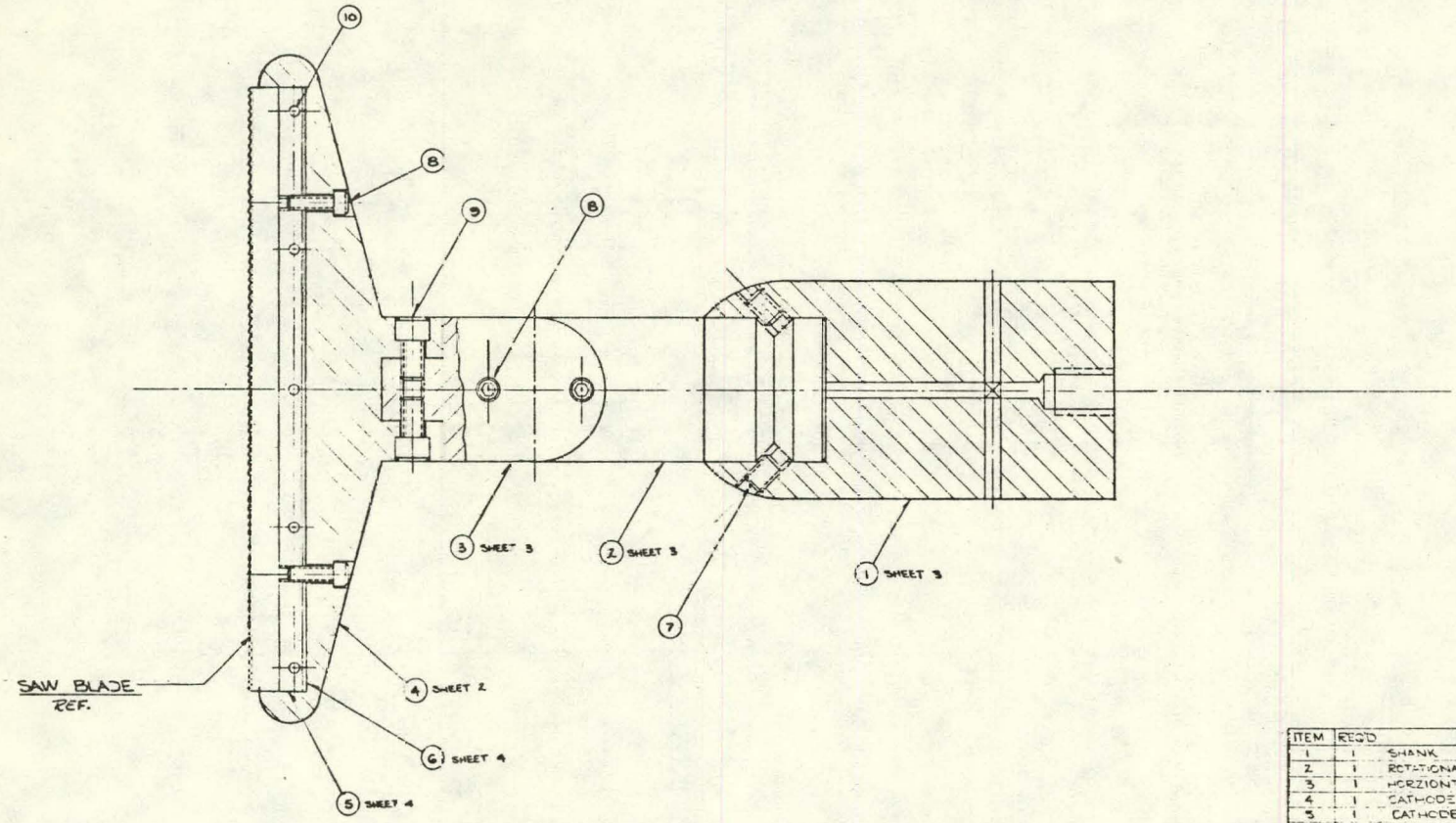

ITEM	REQ'D	DESCRIPTION	SHEET
1	1	SHANK	3
2	1	ROTATIONAL ADAPTER	3
3	1	HORZIONTAL ADAPTER	3
4	1	CATHODE HOLDER	2
5	1	CATHODE TIP BASE	4
6	2	CATHODE TIP RETAINER	4
7	2	3/8-24 NC-2 x 3/4 LG FULL DOG POINT SETSCREW, STEEL	
8	4	1/4-20 NC-2 x 3/4 LG SOC HD CAP SCR., STEEL	
9	2	7/8-16 NC-2 x 5/8 LG SOC HD CAP SCR., STEEL	
10	10	#8-32 NC-2 x 5/16 LG FLAT, SOC HD CAP SCR, STEEL	

Dwg. 8. Cathode Assembly (PPS)

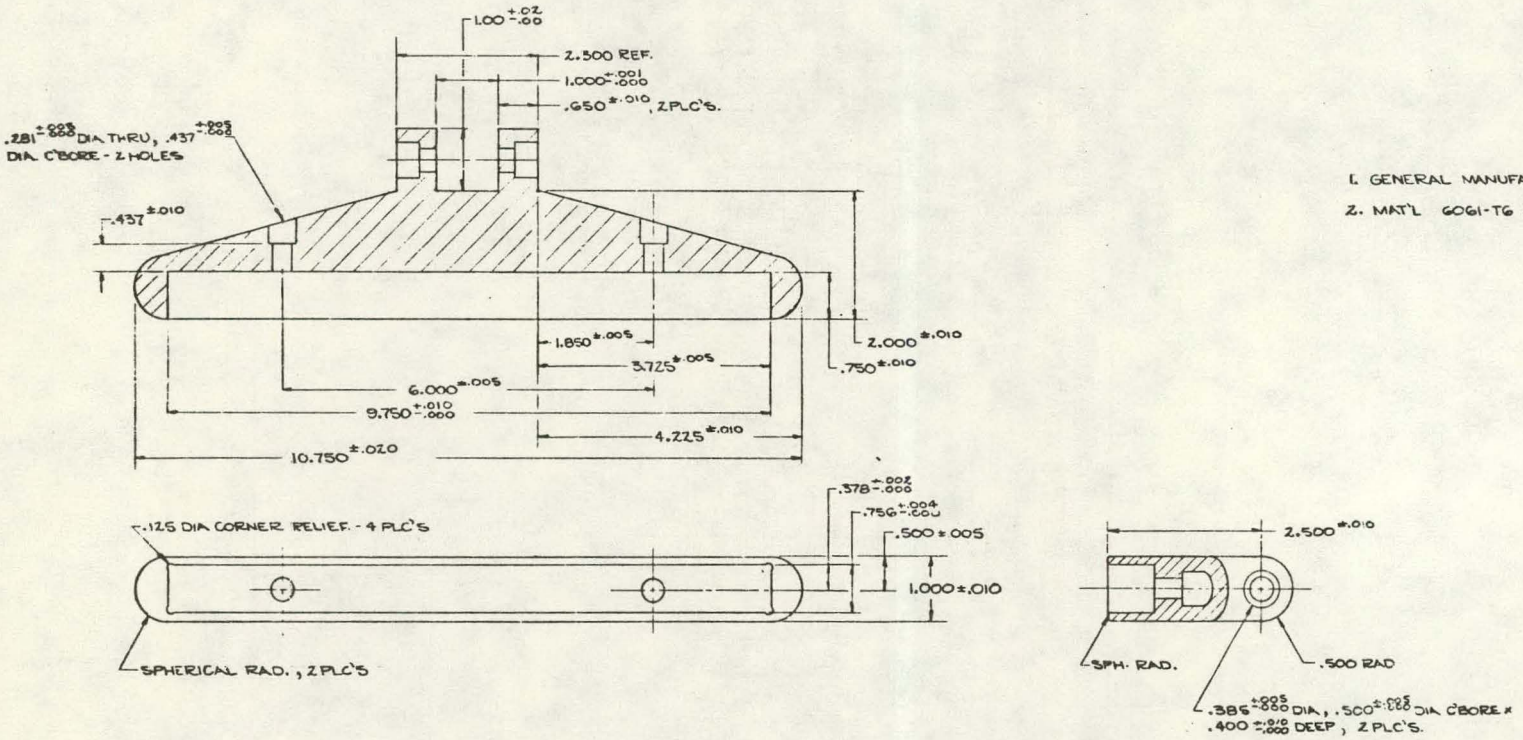

NOTES

1. GENERAL MANUFACTURING INFORMATION 9900000
2. MAT'L GOGI-TG ALUM

ITEM 4

Dwg. 9. Cathode Holder (PPS)

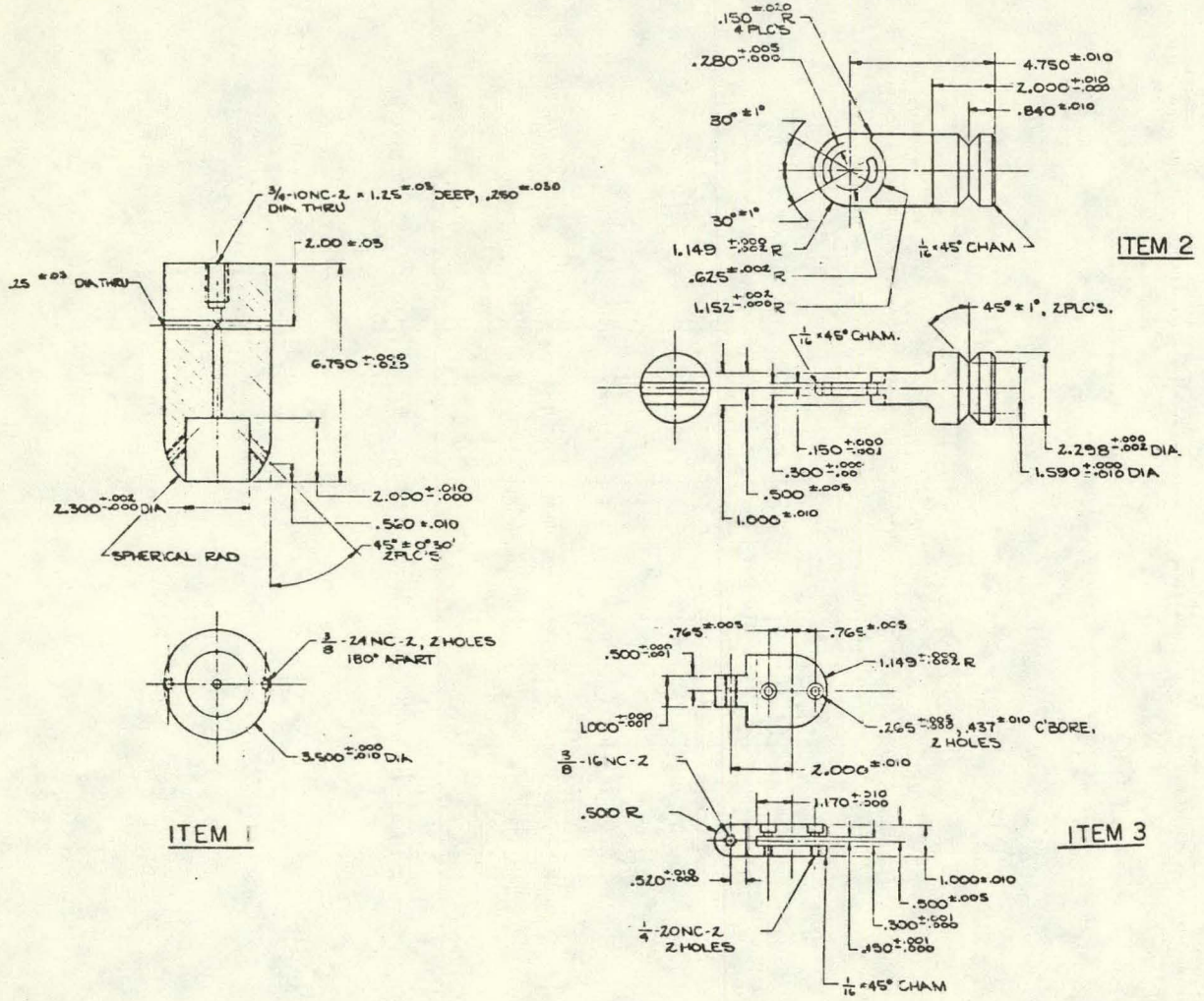

NOTES

1. GENERAL MANUFACTURING INFORMATION 9900000
2. MAT'L: 303 STAINLESS STL.

Dwg. 10. Cathode (PPS)

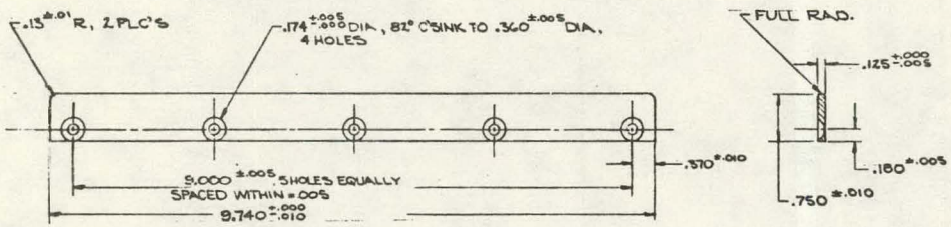

ITEM 6

NOTES

1. GENERAL MANUFACTURING INFORMATION 9900000
2. MAT'L: 303 STAINLESS STL.

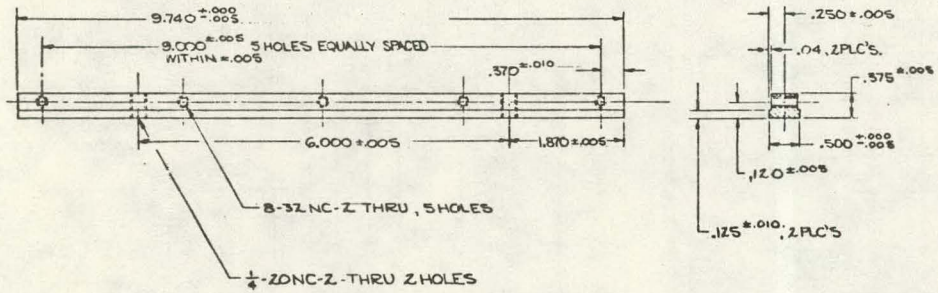

ITEM 5

Dwg. 11. Cathode (PPS)

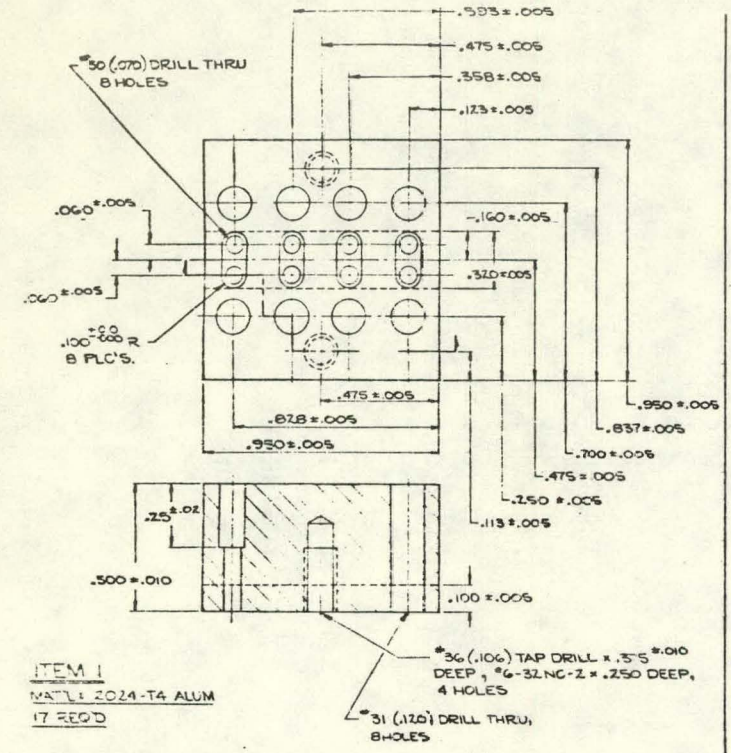

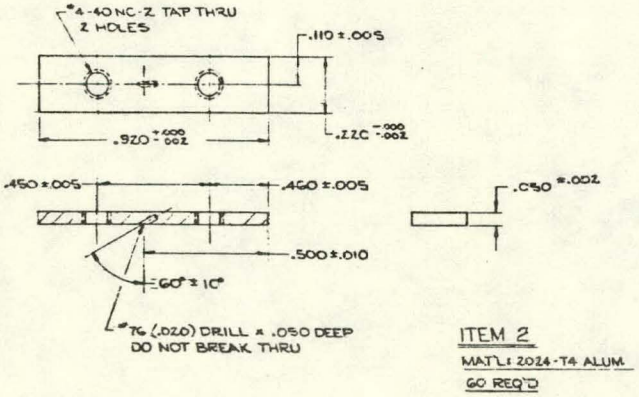

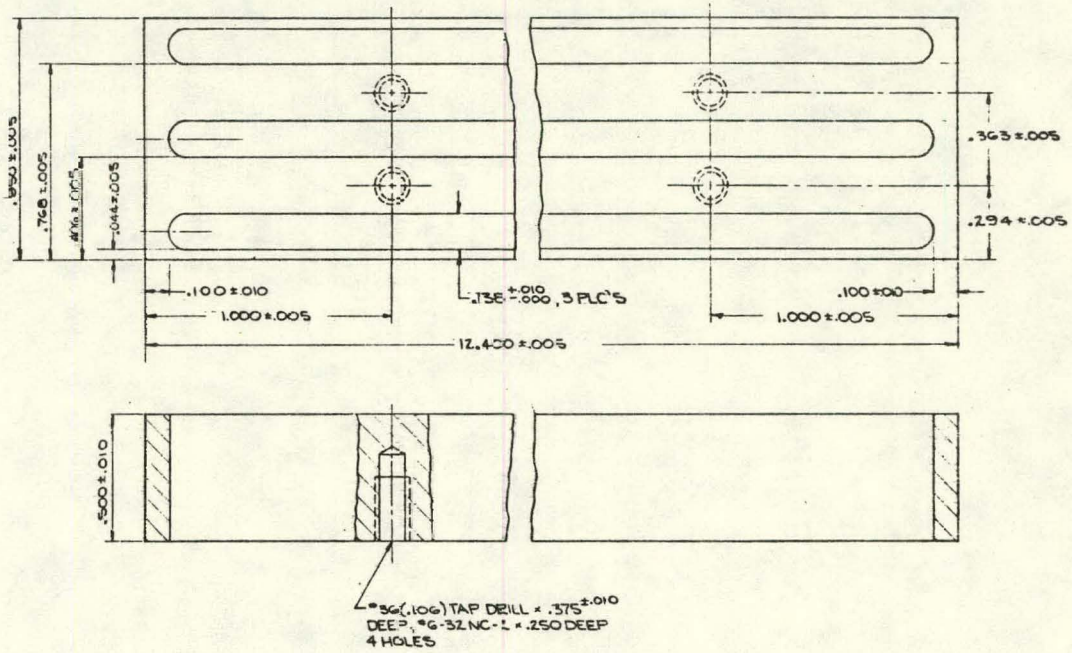

Dwg. 12. Calorimeter (PPS)

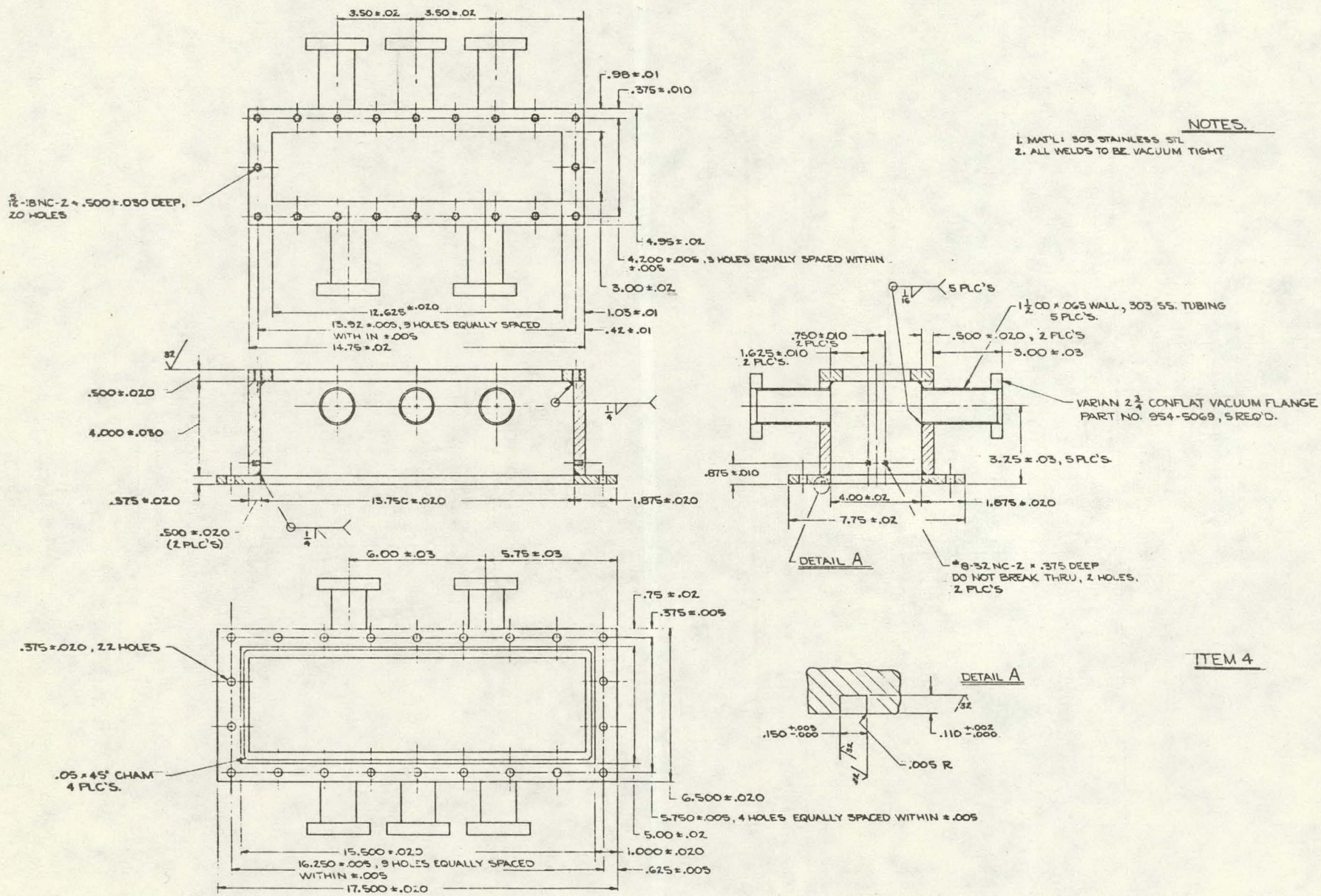

Dwg. 13. Calorimeter Chamber (PPS)

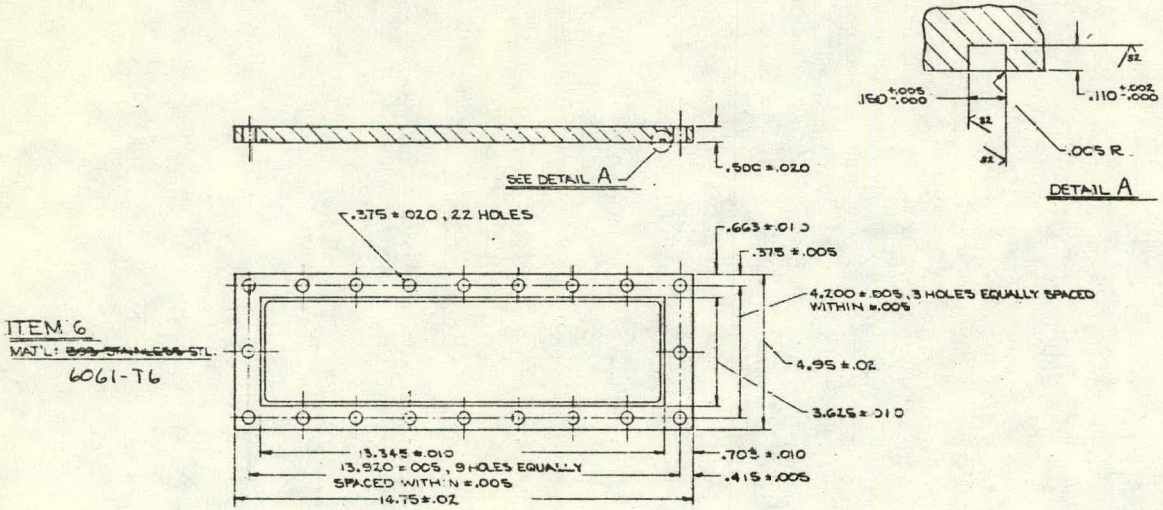

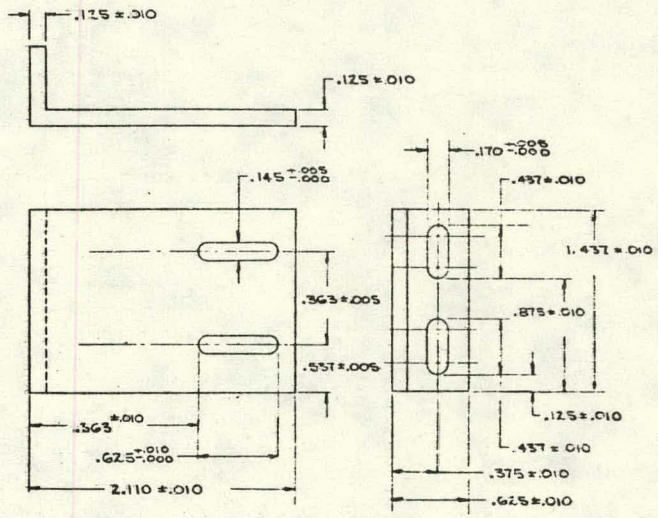

Dwg. 14. Calorimeter (PPS)

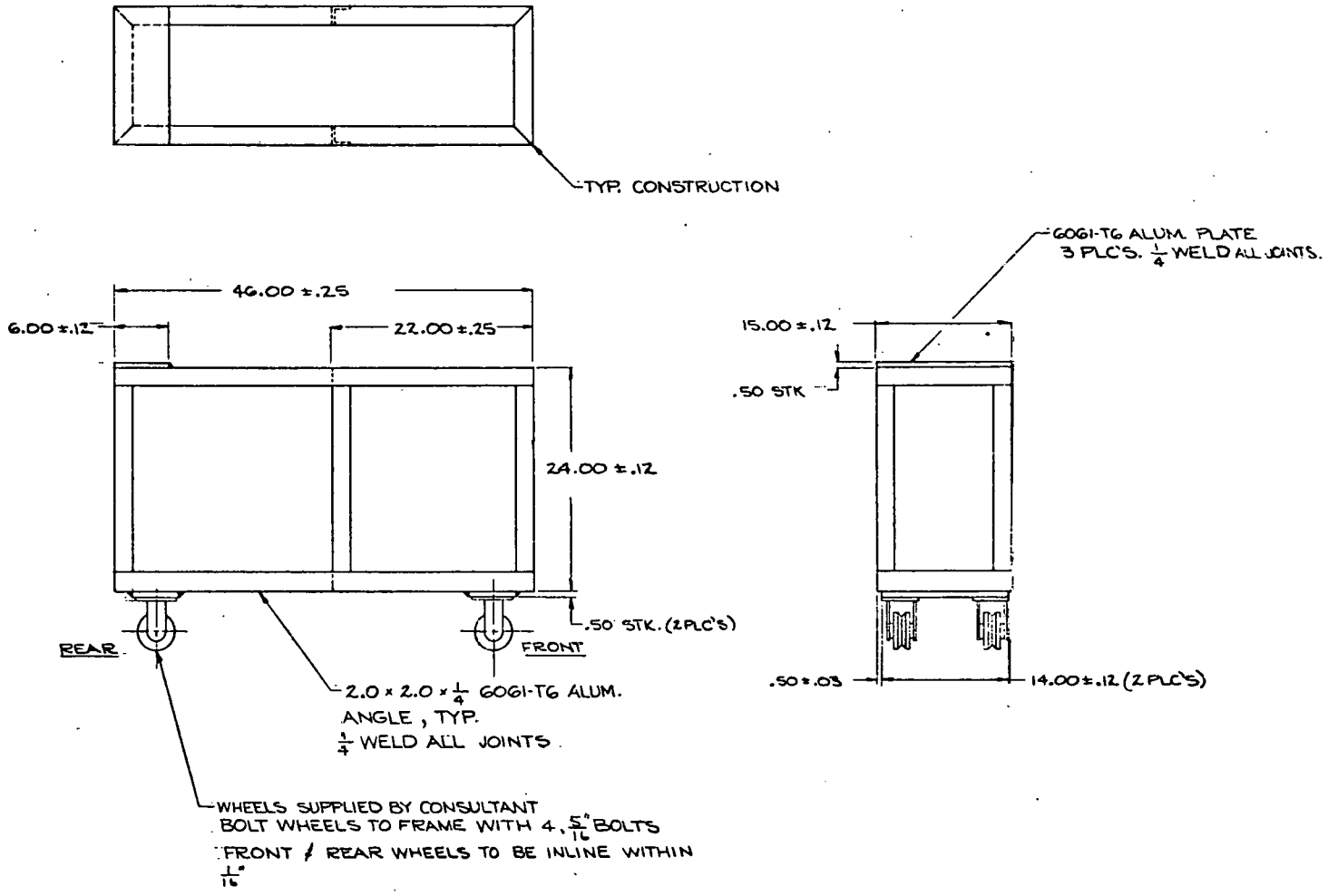

Dwg. 15. Cart (PPS)

UNLIMITED RELEASE

Distribution:

US DOE/NS
Washington, DC 20545
Attn: G. W. Gibbs

University of California
Lawrence Livermore National Laboratory
P. O. Box 808
Livermore, CA 94550
Attn: L. D. Pleasance
E. V. George

Los Alamos Scientific Laboratory
P. O. Box 1663
Los Alamos, NM 87544
Attn: C. Fenstermacher

W. J. Schafer Associates, Inc.
1901 North Ft. Myer Drive
Suite 803
Arlington, VA 22209
Attn: E. Gerry

TRW
1 Space Park
Redondo Beach, CA 90278
Attn: R. Aprahamian

AVCO Everett Research, Inc.
Everett, MA 02149
Attn: J. Daugherty

U. S. Air Force
Air Force Weapons Laboratory
Kirtland AFB, NM 87117
Attn: P. J. Ortwerth, ALC
Maj. S. R. Czyzak

U. S. Naval Research Laboratory
Washington, DC 20390
Attn: S. K. Searles

Maxwell Labs
9244 Balboa Avenue
San Diego, CA 92123
Attn: A. Kolb

Physics International
2700 Merced Street
San Leandro, CA 94577
Attn: J. Martinez

Osaka University
Institute of Laser Engineering
Osaka 565, Japan
Attn: C. Yamanaka

Keio University
Department of Electrical
Engineering
3-14-1 Hiyoshi, Kohoku-Ku
Yokohama 223, Japan
Attn: Tomoo Fujioka
Minoru Obara

4000 A. Narath
4200 G. Yonas
4210 J. B. Gerardo
4211 E. J. McGuire
4212 R. A. Gerber (5)
4212 C. A. Frost
4212 R. A. Hamil
4212 J. M. Hoffman
4212 R. A. Klein (20)
4212 J. B. Moreno
4212 E. L. Patterson
4212 G. E. Samlin
4212 J. H. Stoever
4212 G. C. Tisone
4212 J. R. Woodworth
4214 E. D. Jones
4216 A. W. Johnson
4218 J. K. Rice
4220 M. Cowan
4230 J. E. Powell
4240 G. W. Kuswa
4250 T. H. Martin
4253 K. R. Prestwich
4253 J. J. Ramirez
8266 E. A. Aas
3141 L. J. Erickson (5)
3151 W. L. Garner (3)
(for DOE/TIC)
3154-3 R. P. Campbell (25)

Org.	Bldg.	Name	Rec'd by *	Org.	Bldg.	Name	Rec'd by